Discovery of Selective Inhibitors Targeting Acetylcholinesterase 1 from Disease-Transmitting Mosquitoes

Cecilia Engdahl,[†,$] Sofie Knutsson,[†,$] Fredrik Ekström,[‡] and Anna Linusson[†*]*

[†]Department of Chemistry, Umeå University, SE-901 87 Umeå, Sweden

[‡]Swedish Defense Research Agency, CBRN Defense and Security, SE-906 21 Umeå, Sweden
[*]Corresponding author

[$]These authors contributed equally

E-mail address: anna.linusson@umu.se; fredrik.ekstrom@foi.se

Table of contents

SUPPORTING INFORMATION

Inhibition data from the HTS campaigns against *Ag*AChE1, *Aa*AChE1, and *h*AChE

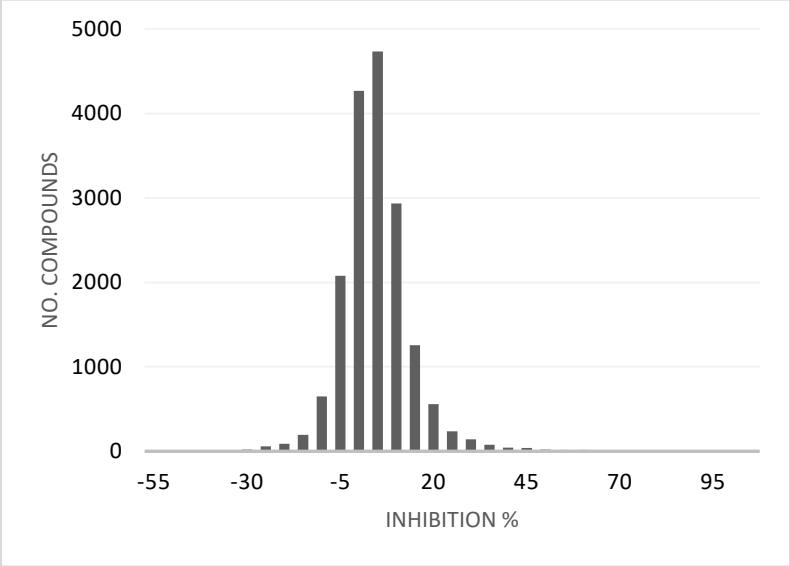

Figure S1. Histogram showing the distribution of the HTS inhibition data for *Ag*AChE1 used in the differential HTS study.

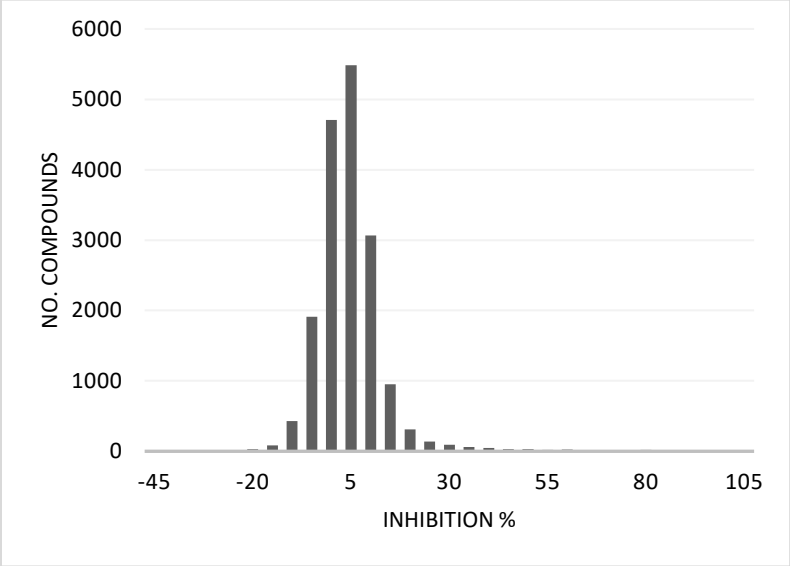

Figure S2. Histogram showing the distribution of the HTS inhibition data for *Aa*AChE1 used in the differential HTS study.

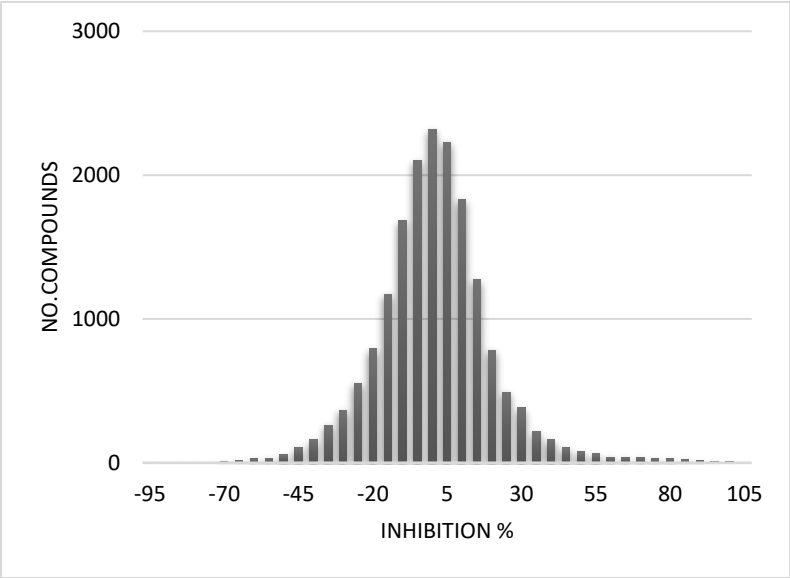

Figure S3. Histogram showing the distribution of the HTS inhibition data for *h*AChE used in the differential HTS study.[1]

Statistics of HTS results

Data was normalized as % of control according to the following equation:

$$\frac{x_i}{\bar{c}_+} \times 100$$

Where

x_i raw measurement

$\bar{c}_+$ mean of eight positive controls within plate (maximum activity)

Table S1. AChE1 HTS statistics based on the screened compounds' inhibition of activity in relation to positive controls.

	***Ag*AChE1**	***Aa*AChE1**
Mean (%)	3	3
Median (%)	2	2
Standard deviation (%)	10	9
Cut-off (%)	33	31
No. of hits	235	286
Hit-rate (%)	1.3	1.6
No. of unique hits of *Ag*AChE1 and/or *Aa*AChE1	**338**	

Reference compounds

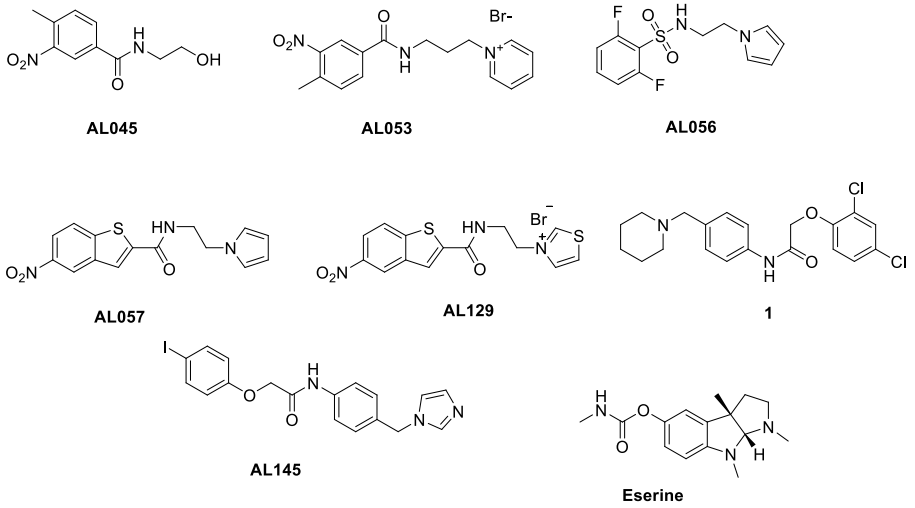

Figure S4. Chemical structures of compounds on reference plate. At 50 µM, these compounds exhibited mean inhibition values ranging from 0-95% for both enzymes, and all but one compound had a standard deviation of 3-8%. The higher standard deviation of the mean observed for compound **1** (17-18%) was probably due to a handling error whereby no compound was added to in total six and three wells of the *Ag*AChE1 and *Aa*AChE1 experiments, respectively.

Reference plate statistics

Table S2. Reference plate statistics.

		AL045	AL053	AL056	AL057	AL129	1	AL145	Eserine
IC_{50}	*Ag*AChE1	1000	62	1000	1000	46	0.26	100	0.005
	*Aa*AChE1	1000	38	1000	1000	37	0.44	100	0.007
mean (%)	*Ag*AChE1[a]	2	18	0	-3	25	90	7	95
	*Aa*AChE1[b]	1	26	0	-3	24	89	11	94
median (%)	*Ag*AChE1[a]	2	19	0	-4	25	93	8	96
	*Aa*AChE1[b]	1	26	0	-4	24	92	10	94
SD	*Ag*AChE1[a]	7	7	8	7	8	18	8	8
	*Aa*AChE1[b]	5	6	6	7	7	17	7	3
total no. of replicates	*Ag*AChE1[a]	216	216	216	216	216	216	216	216
	*Aa*AChE1[b]	96	96	96	96	96	96	96	96
no. scored as hits	*Ag*AChE1[a]	0	7	1	0	19	210	0	215
	*Aa*AChE1[b]	0	14	0	0	9	93	0	96
no. scored as inactive	*Ag*AChE1[a]	216	209	215	216	197	6	216	1
	*Aa*AChE1[b]	96	82	96	96	87	3	96	0

[a]Based on % inhibition from 27 plates with eight replicates/plate [b]based on % inhibition from 12 plates with eight replicates/plate

Z’-factors

a)

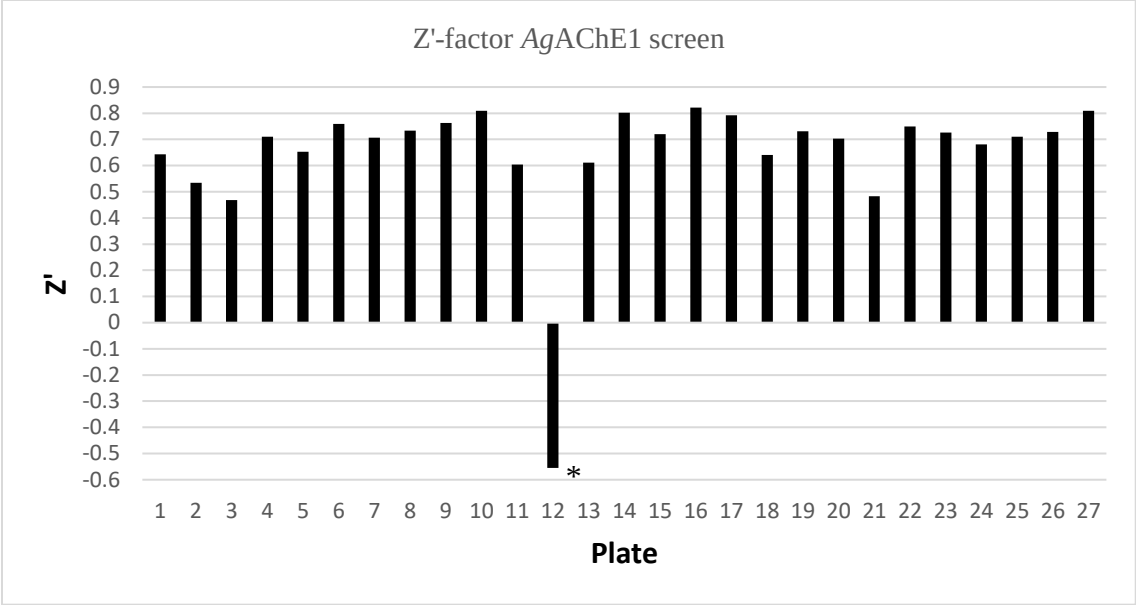

b)

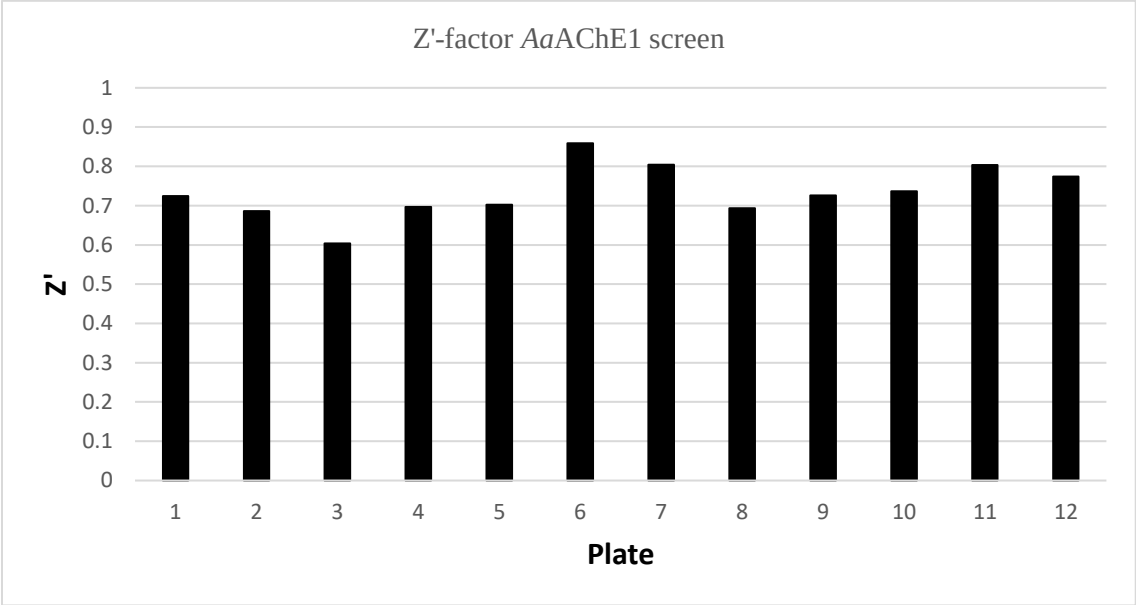

Figure S5. Z’-factors based on eserine and AL045 for each of the reference plate run during the screens against *Ag*AChE1 (a) and *Aa*AChE1 (b). *The negative Z’-factor for this plate was due to one measurement for eserine being an extreme outlier, probably due to a handling error whereby no compound was added to the well (see Figure S5c). Excluding this one measurement resulted in Z’-factor of 0.64 for this plate.

Examples of raw measurements of reference compounds

a)

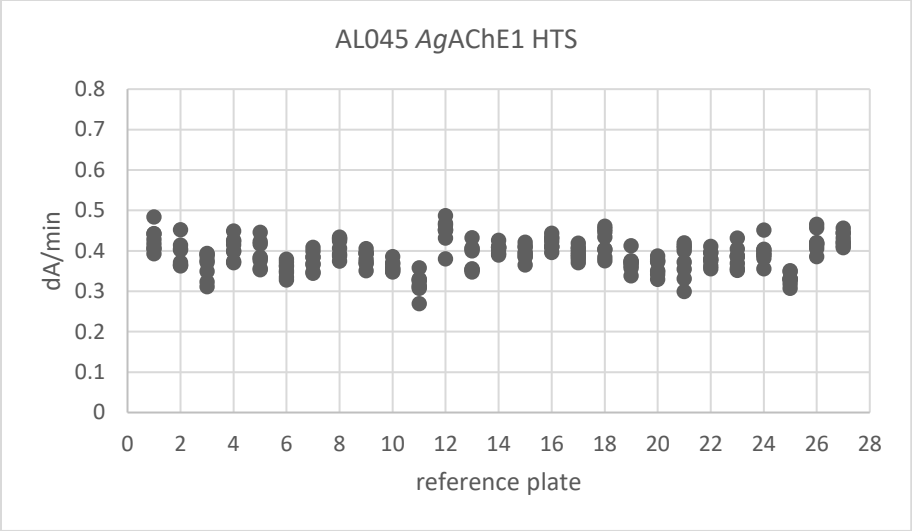

b)

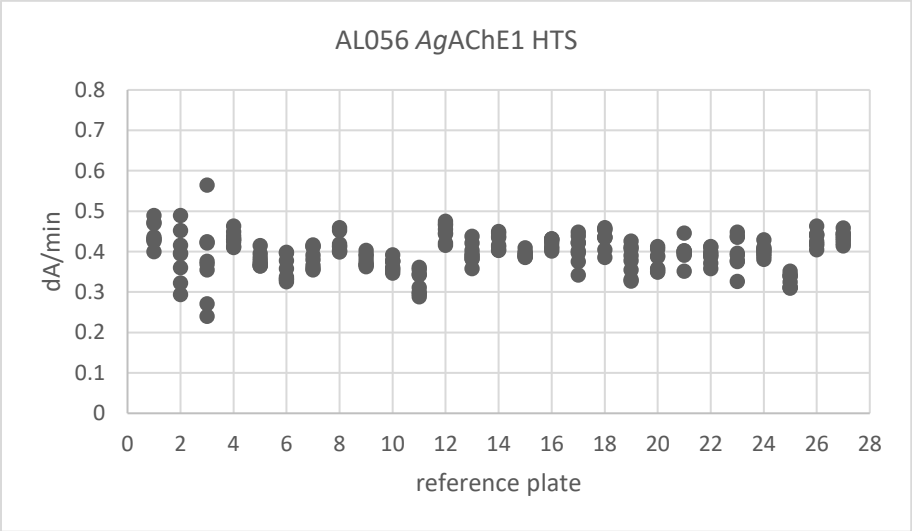

c)

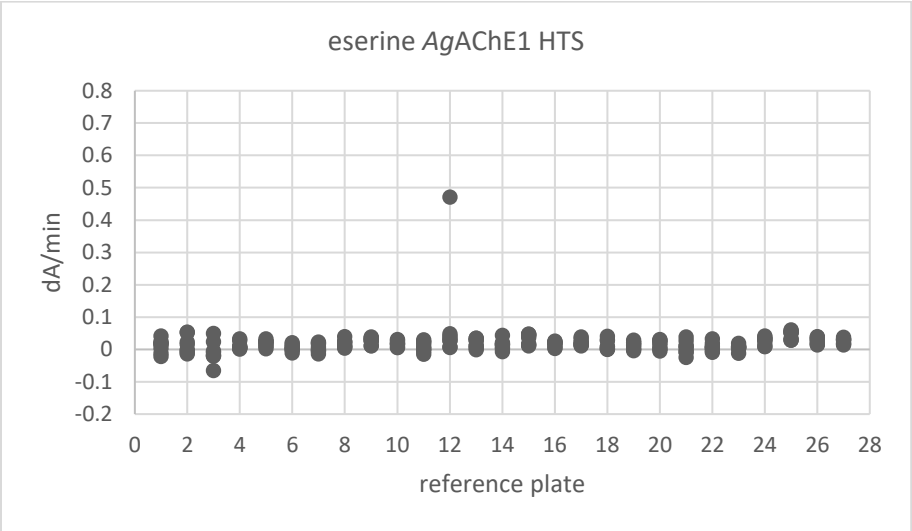

d)

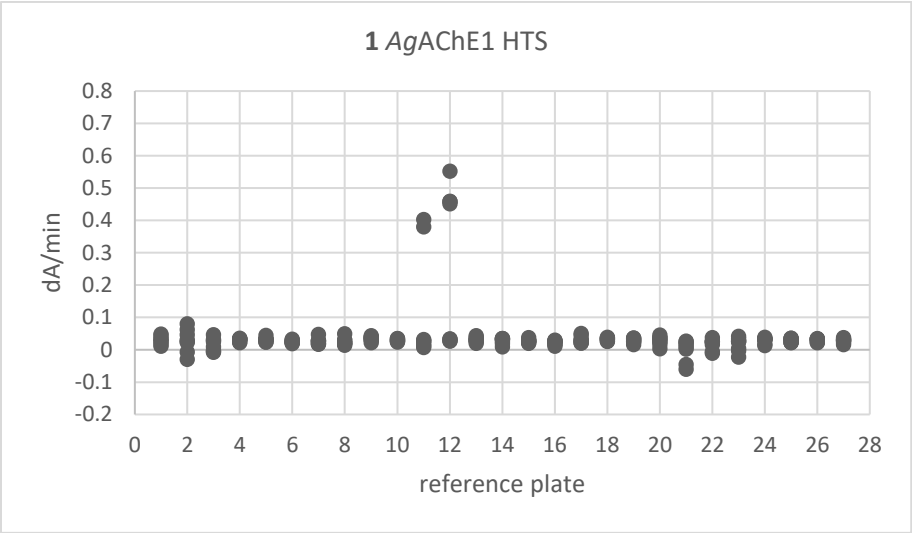

Figure S6. Examples of the change in absorbance over time (dA/min) of four compounds from the reference plate run 27 times during the *Ag*AChE1 screen. Each compound was present in eight replicates on the reference plate. a) Positive control AL045 used for determination of Z'-factor. b) Positive control AL056. C) Negative control eserine used for determination of Z'-factor, one visible outliers (plate 12; dA/min > 0.45) probably due to a handling error whereby no compound was added to that well. d) Negative control **1**, six visible outliers (plate 9 and 12; dA/min > 0.35) probably due to a handling error whereby no compound was added to those wells.

a)

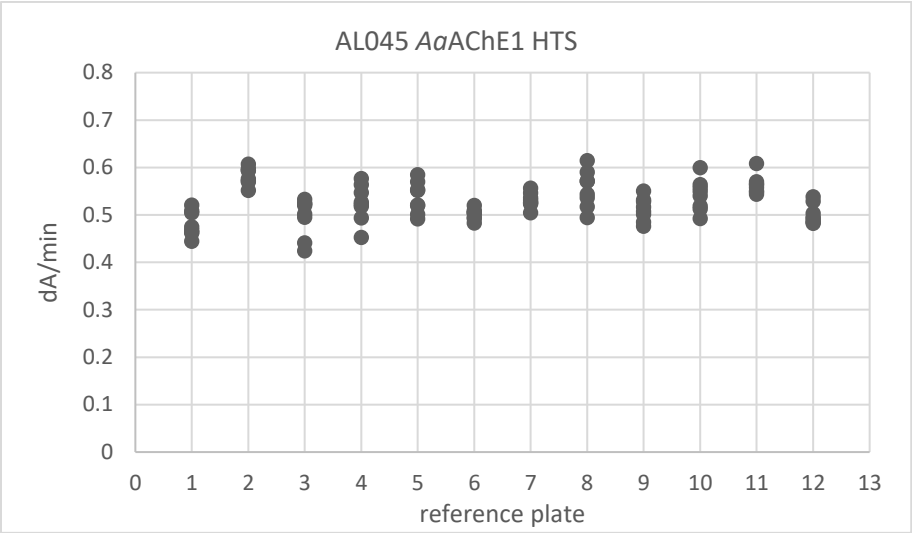
AL045 AaAChE1 HTS
dA/min
0.8
0.7
0.6
0.5
0.4
0.3
0.2
0.1
0
0 1 2 3 4 5 6 7 8 9 10 11 12 13
reference plate

b)

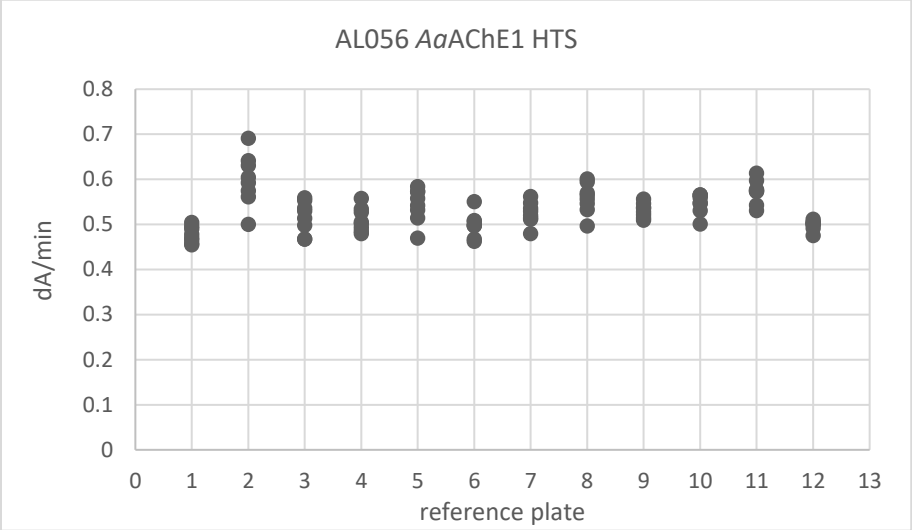
AL056 AaAChE1 HTS
dA/min
0.8
0.7
0.6
0.5
0.4
0.3
0.2
0.1
0
0 1 2 3 4 5 6 7 8 9 10 11 12 13
reference plate

c)

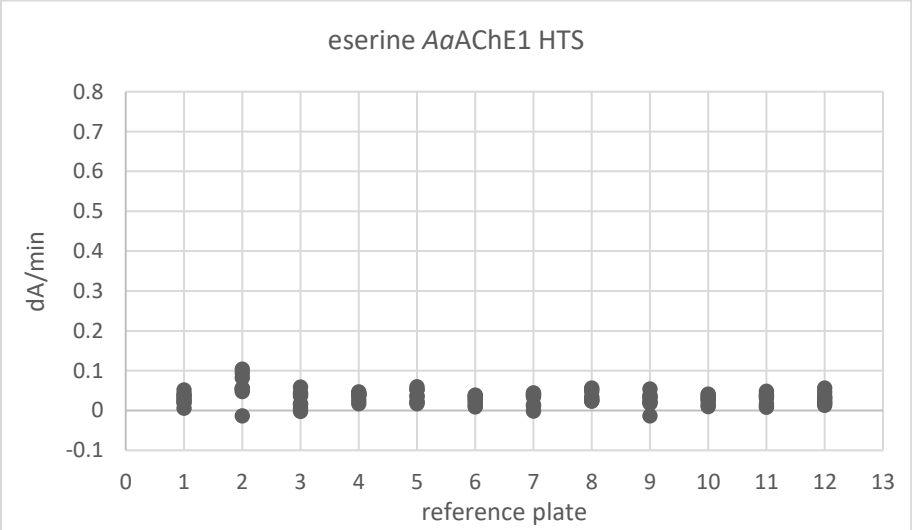
eserine AaAChE1 HTS
dA/min
0.8
0.7
0.6
0.5
0.4
0.3
0.2
0.1
0
-0.1
0 1 2 3 4 5 6 7 8 9 10 11 12 13
reference plate

d)

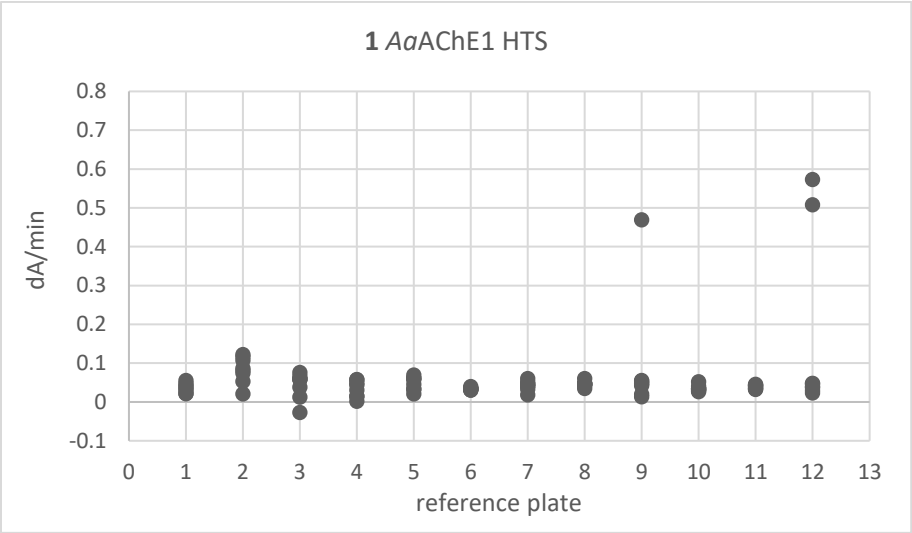

Figure S7. Examples of the change in absorbance over time (dA/min) of four compounds from the reference plate run 12 times during the *Aa*AChE1 screen. Each compound was present in eight replicates on the reference plate. a) Positive control AL045 used for determination of Z'-factor. b) Positive control AL056. C) Negative control eserine used for determination of Z'-factor. d) Negative control **1**, three visible outliers (plate 9 and 12; dA/min > 0.45) probably due to no compound being added to those wells.

Reference plate - Estimation of false positives and false negatives

Table S3. Estimation of false positives and false negatives based on reference plate data for the eight compounds loaded on the reference plate (Figure S3 and Table S2).

	***Ag*AChE1**	***Aa*AChE1**
No. false positives (wells)[a]	27 (6%)	23 (11%)
No. true positives (wells)	425	189
No. false negatives (wells)[b]	7 (0.5%)	3 (0.5%)
No. true negatives (wells)	1269	553

[a]Definition of false positive: a measurement (well) for which reference compound r_i exhibited % inhibition ≥ hit cut-off; where $\bar{r}_i$ < hit cut-off. [b]Definition of false negative: a measurement (well) for which reference compound r_i exhibited % inhibition ≤ hit cut-off; where $\bar{r}_i$ > hit cut-off.

Overview of the PCA models describing the AChE1 hits

Table S4. Model statistics of principal component analysis (PCA) used to describe and visualize the chemical diversity of the AChE1 hits and selection of compounds for IC_{50} determinations. PCA is an unsupervised regression method used here to extract the main variation in the 2D-descriptor data (i.e. principal components). The PCA models were calculated on mean-centered data scaled to unit variance using software SIMCA-P+[2] and the number of significant components for each model were determined using scree-plots.

	Model	No of hits	No of descriptors	No of components	Eigenvalue of last component	R^2X (cum)	Q^2X (cum)
1	all AChE1 hits	338	73	4	3.72	0.85	0.82
2	hits ≥ 70% inhibition	55	73	4	3.42	0.83	0.74
3	hits 69-31% inhibition	248	73	4	3.61	0.86	0.83
4	hits ≥ 30% difference between *Aa*- and *Ag*AChE1	35	73	3	3.88	0.84	0.78
5	hit sets A and B	47	73	3	7	0.83	0.74

Table S5. Physicochemical descriptors used to describe the chemical space spanned by the AChE1 hits. The 2D-descriptors were calculated using MOE[3] on structures prepared as described in the Experimental section.

No.	Descriptor	No.	Descriptor	No.	Descriptor
1	**apol**	26	**chi0_C**	51	**PEOE_VSA_NEG**
2	**a_acc**	27	**chi1**	52	**PEOE_VSA_PNEG**
3	**a_aro**	28	**chi1v**	53	**PEOE_VSA_POL**
4	**a_count**	29	**chi1v_C**	54	**PEOE_VSA_POS**
5	**a_donacc**	30	**chi1_C**	55	**PEOE_VSA_PPOS**
6	**a_heavy**	31	**density**	56	**radius**
7	**a_hyd**	32	**diameter**	57	**rings**
8	**a_IC**	33	**Kier1**	58	**SlogP**
9	**a_ICM**	34	**Kier2**	59	**SMR**
10	**a_nC**	35	**Kier3**	60	**TPSA**
11	**a_nH**	36	**KierA1**	61	**VAdjEq**
12	**a_nO**	37	**KierA2**	62	**VAdjMa**
13	**balabanJ**	38	**KierA3**	63	**VDistEq**
14	**bpol**	39	**KierFlex**	64	**VDistMa**
15	**b_1rotN**	40	**logS**	65	**vdw_area**
16	**b_1rotR**	41	**PEOE_PC+**	66	**vdw_vol**
17	**b_ar**	42	**PEOE_PC-**	67	**vsa_hyd**
18	**b_count**	43	**PEOE_RPC-**	68	**vsa_other**
19	**b_heavy**	44	**PEOE_VSA_FHYD**	69	**vsa_pol**
20	**b_rotN**	45	**PEOE_VSA_FNEG**	70	**Weight**
21	**b_rotR**	46	**PEOE_VSA_FPNEG**	71	**weinerPath**
22	**b_single**	47	**PEOE_VSA_FPOL**	72	**weinerPol**
23	**chi0**	48	**PEOE_VSA_FPOS**	73	**zagreb**
24	**chi0v**	49	**PEOE_VSA_FPPOS**		
25	**chi0v_C**	50	**PEOE_VSA_HYD**		

Chemical space of AChE1 hits

a)

b)

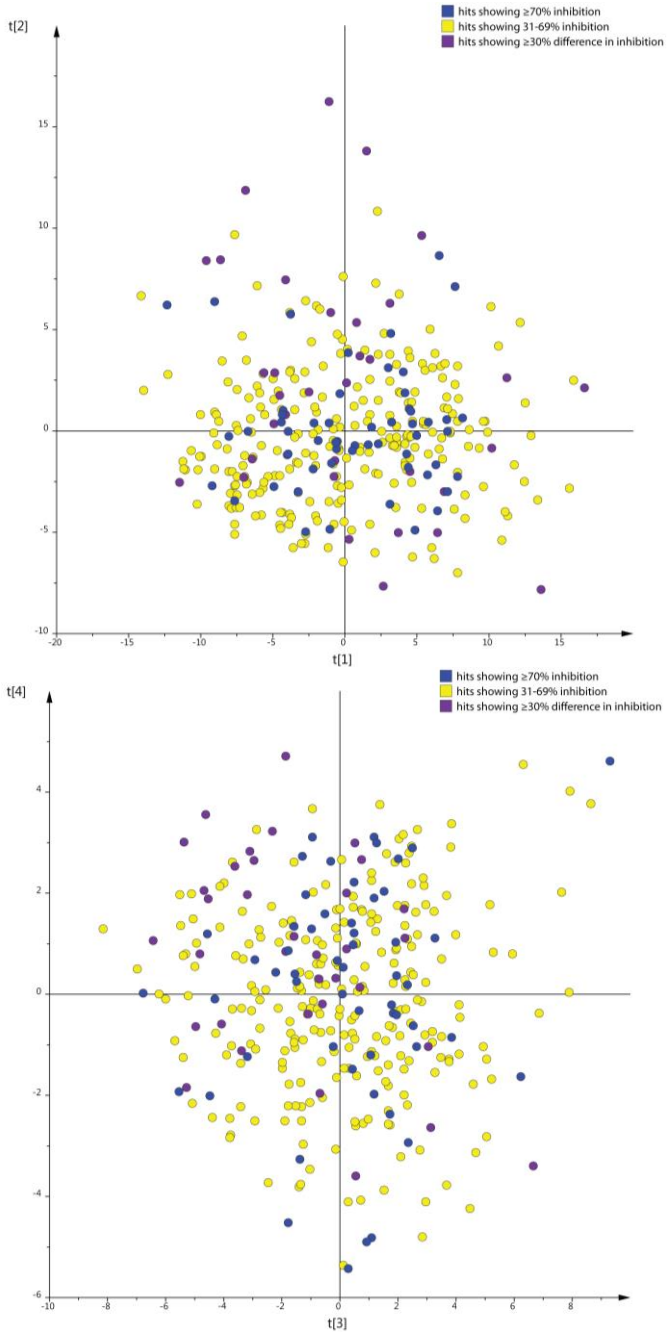

Figure S8. Chemical space of AChE1 hits. Score plots from PCA of the physicochemical properties of the identified hits colored according to their inhibition in the HTS. Hits with ≥ 70% inhibition in blue, 31-69% inhibition in yellow, and hits with ≥ 30% difference inhibition between *Aa*- and *Ag*AChE1 in purple. The first and second components describe the size and hydrophobicity of the hits (a) and the third and fourth components show diversity relating to flexibility and charge (b).

a)

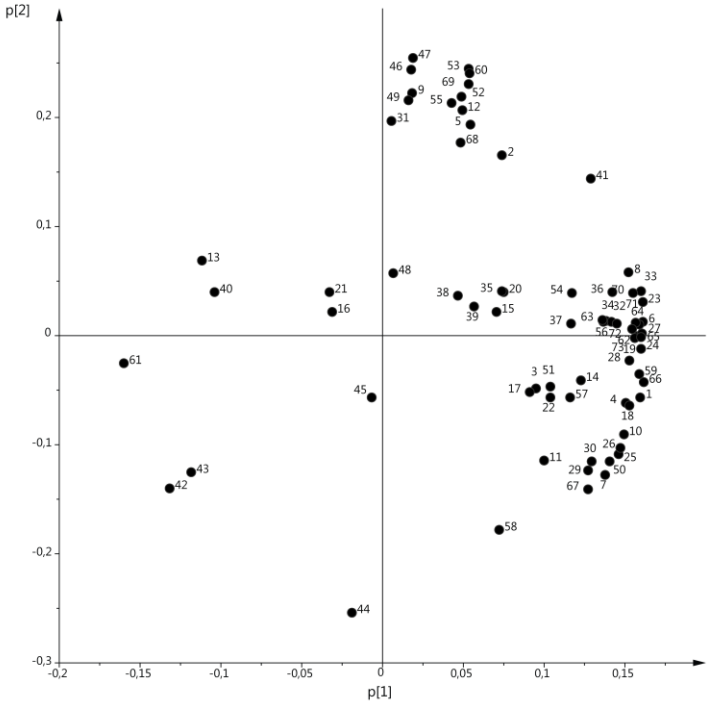

b)

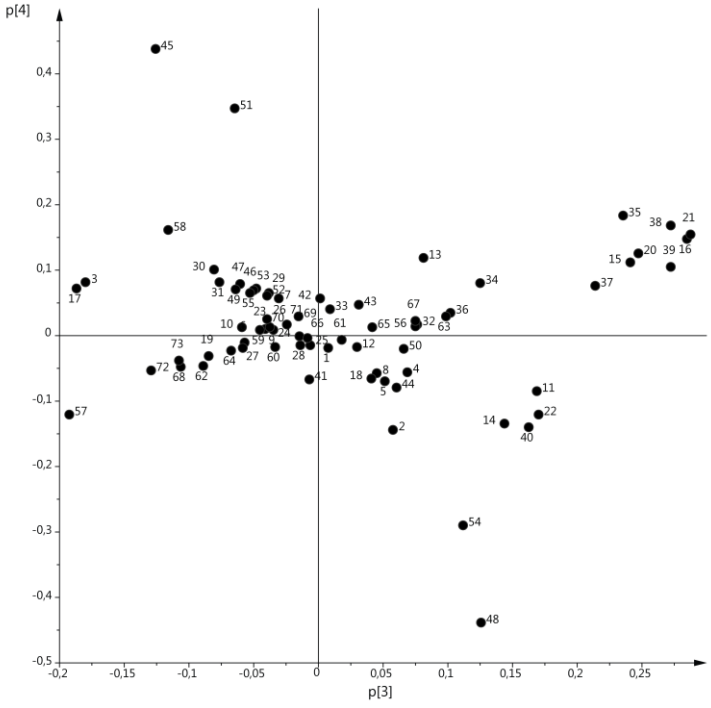

Figure S9. Chemical space of AChE1 hits. PCA loading plots of (a) p1 versus p2 and (b) p3 versus p4. The physicochemical descriptors included in the model are labeled with the numbers assigned in Table S5.

Selection of compounds for IC_{50} determination

a)

b)

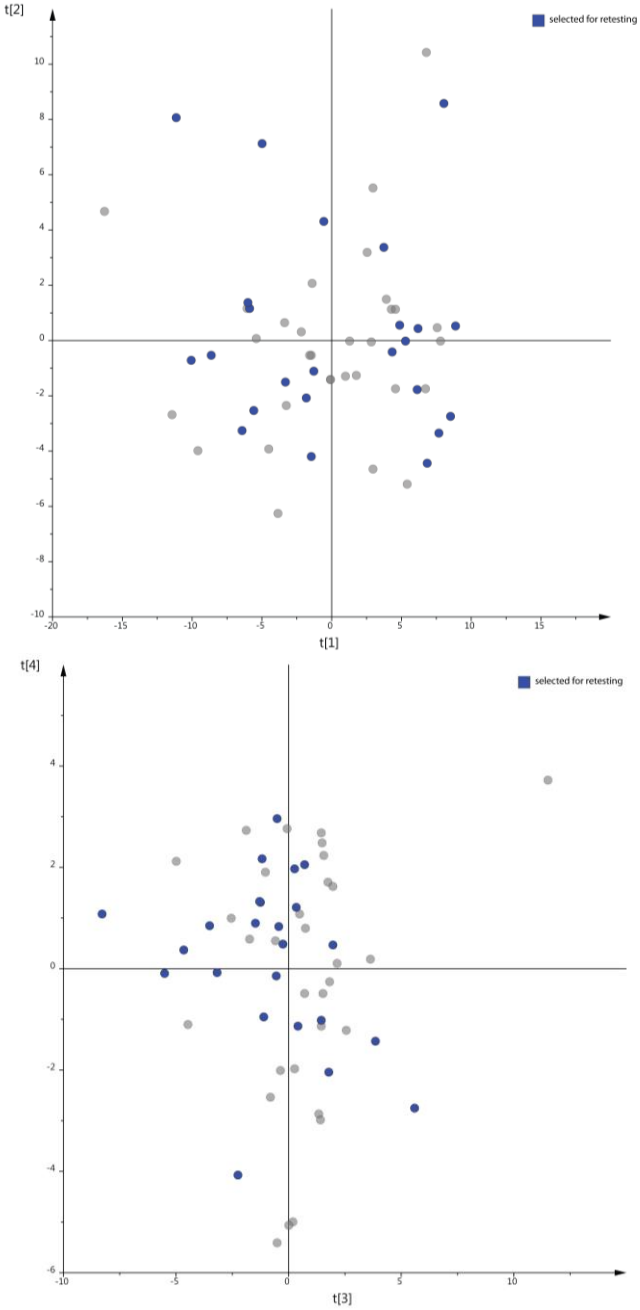

Figure S10. Chemical space of AChE1 hits showing ≥ 70% inhibition. Score plots from PCA of the physicochemical properties of the 55 hits showing at least 70% inhibition in the HTS, hits manually selected for IC_{50} determination colored in blue (set A). The first and second components describe the size and hydrophobicity of the hits (a) and the third and fourth components show diversity relating to flexibility and charge (b).

a)

b)

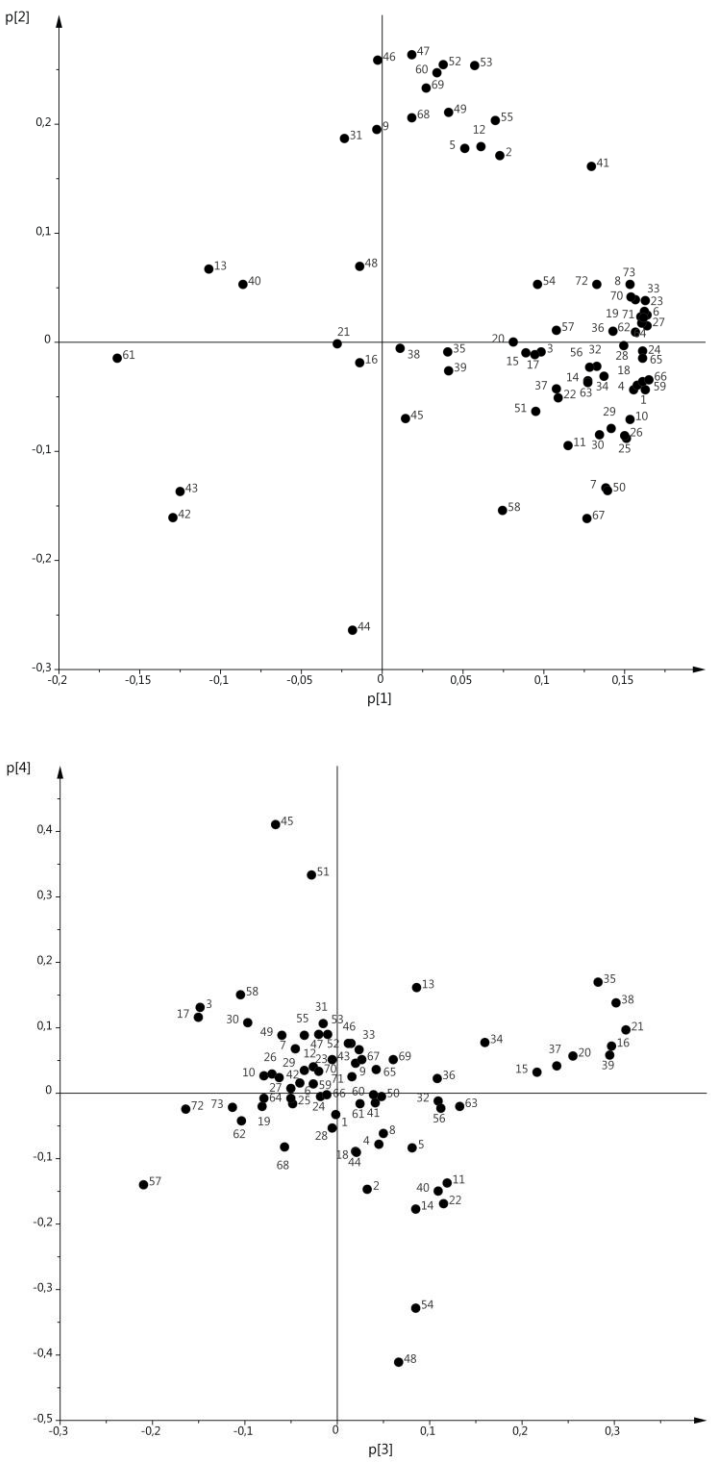

Figure S11. Chemical space of AChE1 hits showing ≥ 70% inhibition. PCA loading plots of (a) p1 versus p2 and (b) p3 versus p4. The physicochemical descriptors included in the model are labeled with the numbers assigned in Table S5.

a)

b)

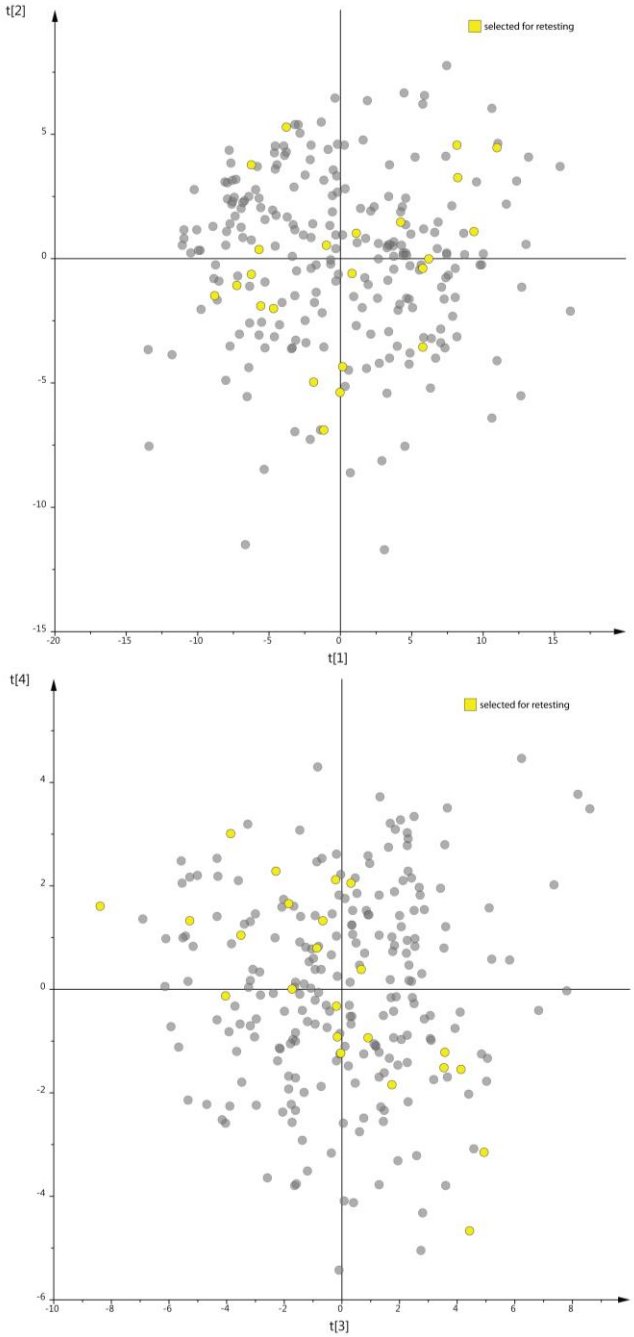

Figure S12. Chemical space of AChE1 hits showing 31-69% inhibition. Score plots from PCA of the physicochemical properties of the 248 hits showing at least 31-69% inhibition in the HTS, hits manually selected for IC_{50} determination colored in yellow (set B). The first and second components describe the size and hydrophobicity of the hits (a) and the third and fourth components show diversity relating to flexibility and charge (b).

a)

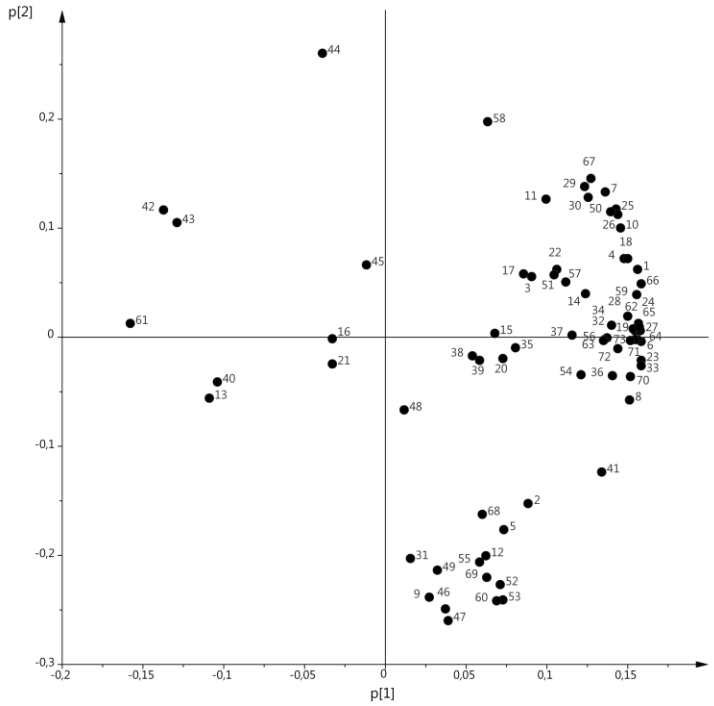

b)

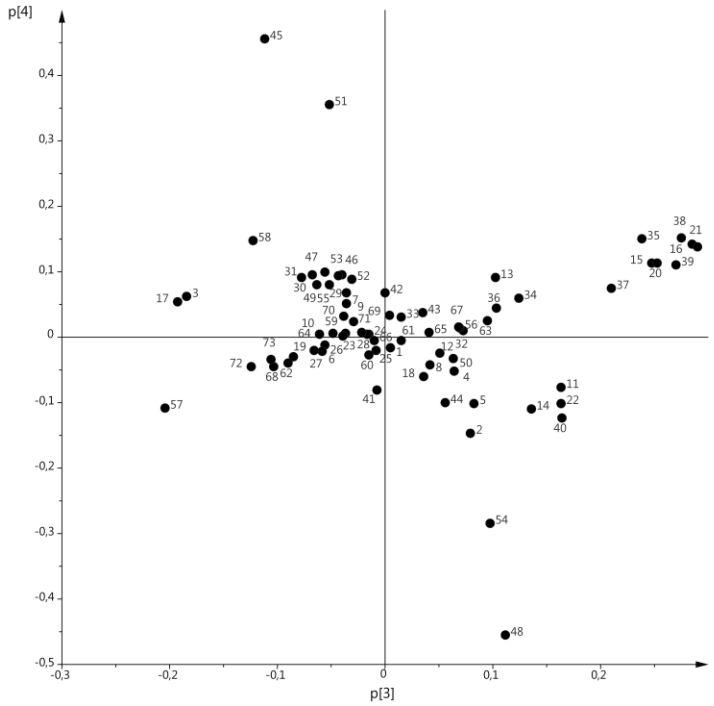

Figure S13. Chemical space of AChE1 hits showing 31-69% inhibition. PCA loading plots of (a) p1 versus p2 and (b) p3 versus p4. The physicochemical descriptors included in the model are labeled with the numbers assigned in Table S5.

a)

b)

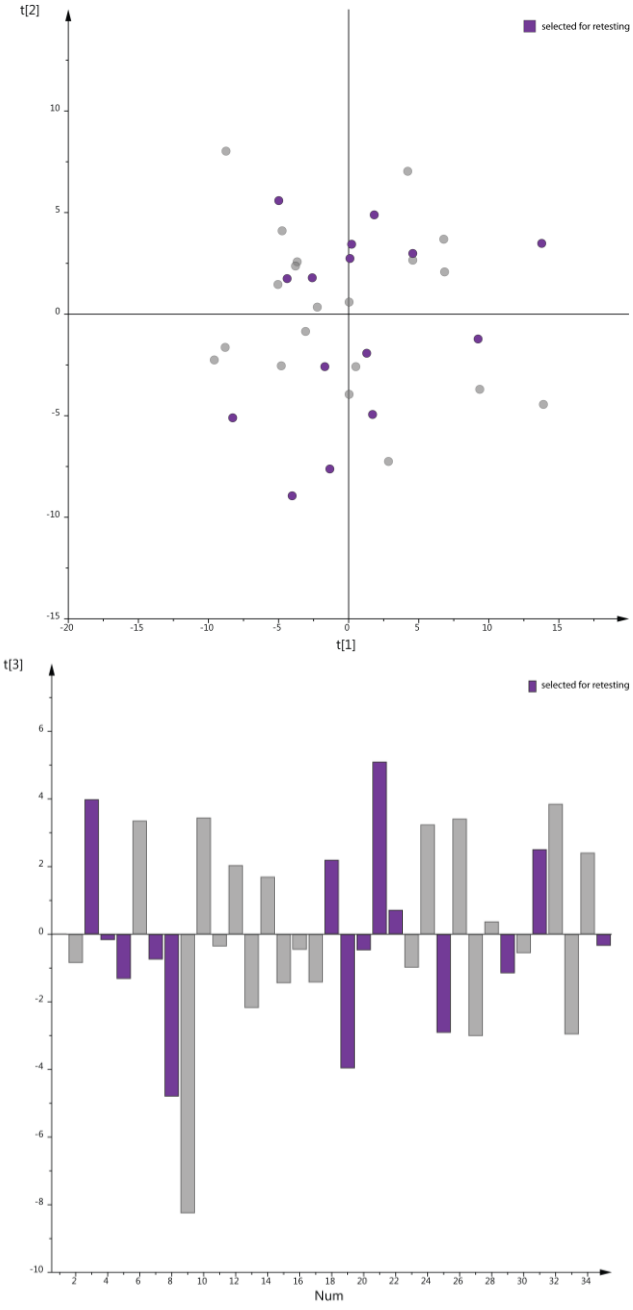

Figure S14. Chemical space of AChE1 hits showing ≥ 30% difference in inhibition between *Ag*- and *Aa*AChE1. PCA of the physicochemical properties of the 35 hits showing at least 30% difference in inhibition between *Aa*- and *Ag*AChE1 in the HTS, hits manually selected for IC_{50} determination colored in purple (set D1 and D2). The first and second components describe the size and hydrophobicity of the hits (a) and the third component shows diversity relating to flexibility (b).

a)

b)

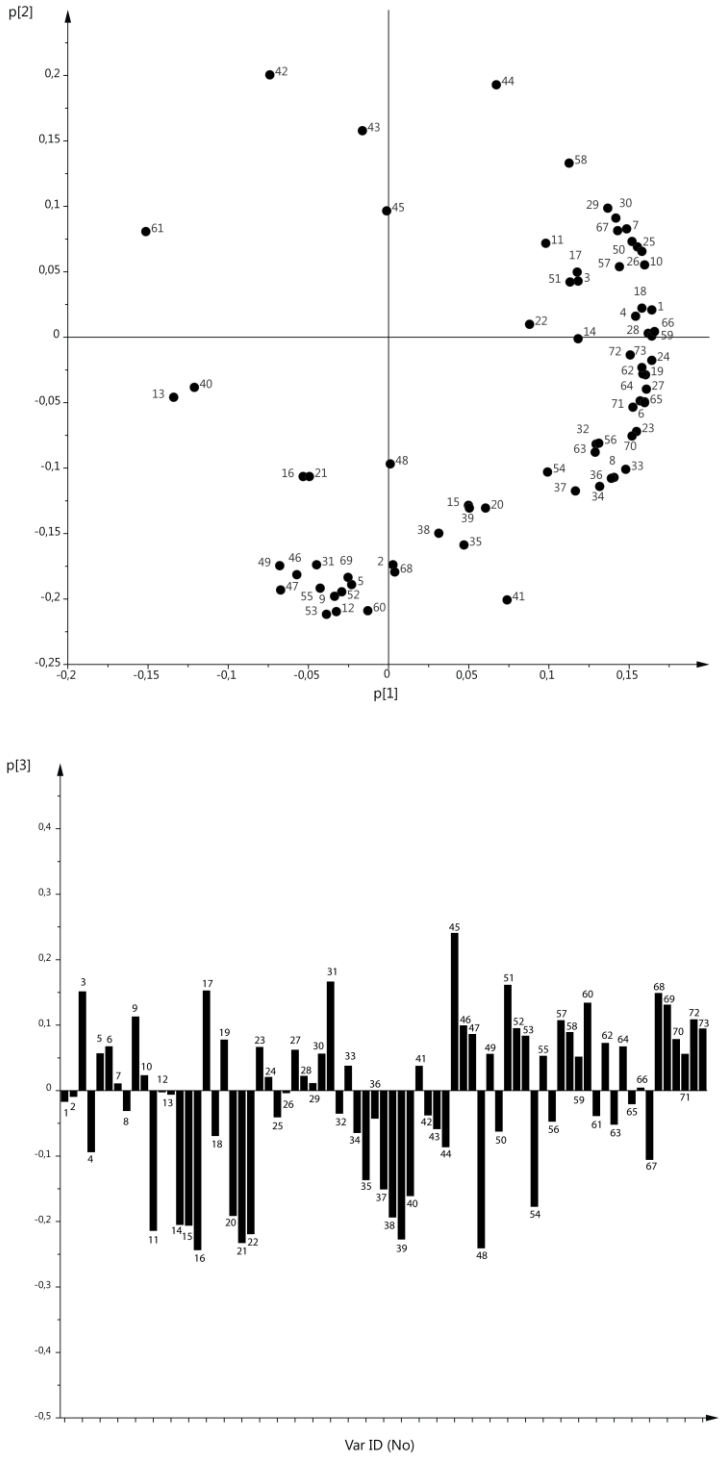

Figure S15. Chemical space of AChE1 hits showing ≥ 30% difference in inhibition between *Ag*- and *Aa*AChE1. PCA loading plots of (a) p1 versus p2 and (b) p3. The physicochemical descriptors included in the model are labeled with the numbers assigned in Table S5.

a)

b)

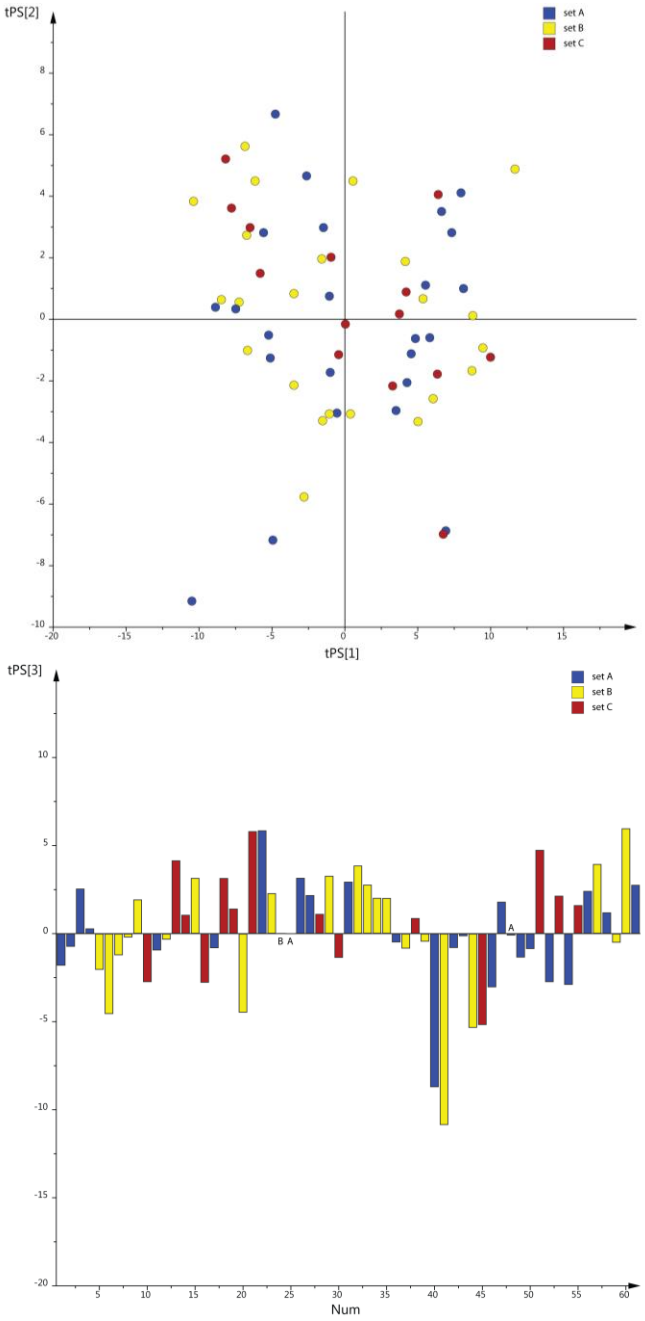

Figure S16. Chemical space of AChE1 hits in sets A and B. Score plots from PCA of the physicochemical properties of the 47 hits in sets A (blue) and B (yellow) selected for IC_{50} determinations. Compounds of set C (≤ 30% inhibition; red) were manually selected from compounds with similar structures and physicochemical properties as the compounds in set A and B and have here been projected into the chemical space. The first and second components describe the size and flexibility of the hits (a) and the third component shows diversity relating to polarity and charge (b).

a)

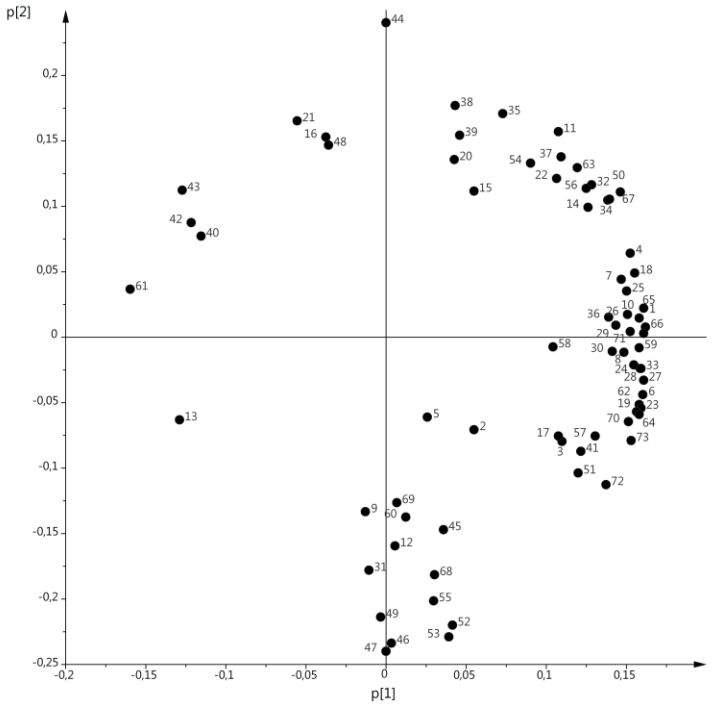

b)

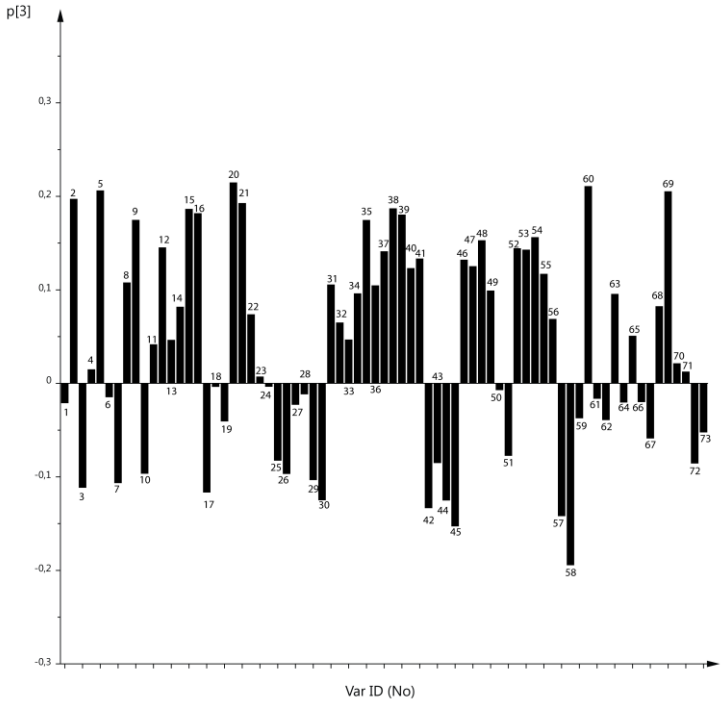

Figure S17. Chemical space of AChE1 hits in sets A and B. PCA loading plots of (a) p1 versus p2 and (b) p3. The physicochemical descriptors included in the model are labeled with the numbers assigned in Table S5.

Complete inhibition results for all the re-tested compounds

Table S6. The complete inhibition results for all the re-tested compounds.

		HTS (%)			IC_{50} (μM)[a]			% activity at 200 μM[b]			S.R.	
ID	**set**	***Ag*AChE1**	***Aa*AChE1**	***h*AChE[c]**	***Ag*AChE1**	***Aa*AChE1**	***h*AChE**	***Ag*AChE1**	***Aa*AChE1**	***h*AChE**	**HTS[d]**	**IC_{50}[e]**
2	A	92	76	12	0.21	0.22	31				6.3	141
3	A	86	90	33	>100	>100	>200	50	49	71	2.6	
4	A	94	93	56	8	9	5				1.7	0.6
5	A	76	82	-12	>1000	>1000	>1000	84	91	78	76	
C0076	A	81	78	-14	>1000	>1000	>1000	87	96	92	78	
C0147	A	94	95	2	0.7	0.8	>200			45	47	>250
C0656	A	69	79	-1	2	2	80				69	40
C0710	A	88	88	57	0.7	0.7	7				1.5	10
C1457	A	87	89	66	0.4	0.3	5				1.3	13
C2681	A	86	88	-11	1	1	>1000			88	86	>1000
C2810	A	89	93	6	1	2	>200			58	14.8	>100
C3029	A	74	78	-16	3	3	>1000			80	74	>333
C4127	A	92	96	85	0.4	0.4	3				1.1	7.5
C4514	A	92	78	-9	10	9	>200			56	67	>20
C4584	A	76	72	7	16	6	>1000			91	10.3	>63
C5063	A	91	81	-11	2	1	72				81	36
C5651	A	96	95	83	5	4	3				1.1	0.6
C6233	A	86	82	28	86	66	>1000			83	2.9	>12
C6483	A	86	89	9	4	4	>300			84	9.6	>75
C7066	A	74	78	-17	6	3	>1000			80	74	>167
C8319	A	80	78	81	5	5	2				1	0.4
C8405	A	92	88	-3	1	1	>200			65	88	>200
C9464	A	86	90	-1	4	3	>300			71	86	>75
C9940	A	61	72	17	2	2	10				3.6	5
6	B	23	38	-7	>500	>500	>500	80	86	81	23	
7	B	32	33	3	17	12	>200			58	11	>12
C0269	B	48	49	-4	9	9	>1000			86	48	>111
C1687	B	13	36	57	>200	>200	19	54	49		0.2	<0.1
C1815	B	22	48	70	n.d.	n.d.	n.d.				0.3	
C1844	B	34	37	31	7	6	13				1.1	2
C2599	B	46	58	-5	22	19	>400			58	46	>18
C2972	B	66	63	-2	9	9	>1000			68	63	>111
C3732	B	24	43	3	11	12	129				8	11
C3922	B	56	0	15	>300	>300	>300	72	54	63	3.7	
C4233	B	47	30	37	>1000	>1000	>1000	70	79	63	0.8	
C4790	B	44	50	1	n.d.	n.d.	n.d.				44	

Table S6. Continued.

		HTS (%)			IC_{50} (μM)[a]			% activity at 200 μM[b]			S.R.	
ID	**set**	***Ag*AChE1**	***Aa*AChE1**	***h*AChE[c]**	***Ag*AChE1**	***Aa*AChE1**	***h*AChE**	***Ag*AChE1**	***Aa*AChE1**	***h*AChE**	**HTS[d]**	**IC_{50}[e]**
C5737	B	65	67	0	5	6	>100			48	65	>17
C6103	B	46	51	22	6	5	>100			45	2.1	>17
C6176	B	57	66	81	8	10	12				0.7	1
C6727	B	53	53	-5	7	4	>100			40	53	>14
C7129	B	47	56	6	11	11	>500			80	7.8	>45
C7786	B	39	45	18	5	6	>300			55	2.2	>50
C7920	B	37	41	6	>400	>400	>400	62	59	79	6.2	
C7951	B	58	53	32	n.d.	n.d.	n.d.				1.7	
C8584	B	34	25	10	n.d.	n.d.	n.d.				2.5	
C8678	B	41	57	19	>1000	>1000	>1000	91	83	98	2.2	
C9503	B	57	69	12	2	2	47				4.8	24
8	C	24	18	2	21	19	43				9	2
C0459	C	3	8	-33	>1000	>500	>500	94	61	73	3	
C0890	C	5	-5	90	>1000	>1000	>1000	109	101	96	0	
C1234	C	1	8	84	>1000	>1000	>100	97	114	45	0	
C1409	C	4	13	-28	69	54	>1000	41	37	81	4	14
C3666	C	10	5	0	>1000	>1000	>200	86	76	54	5	
C4098	C	-10	-11	84	>1000	>1000	>100	62	94	44	0	
C5156	C	-21	-10	95	11	12	0.6				0	0.05
C5504	C	2	-3	-20	n.d.	n.d.	n.d.				1	
C7422	C	16	25	-3	73	128	>600			70	16	>5
C8086	C	6	13	20	>100	>100	>500	47	43	79	0.3	
C9083	C	-1	-1	-6	n.d.	n.d.	n.d.				1	
C9395	C	0	-9	-15	>1000	>1000	>1000	102	98	93	1	
C9657	C	2	2	3	>1000	>1000	>200	85	86	58	0.7	
9	D1	63	1	-14	>1000	>1000	>1000	92	105	86	1	
C0273	D1	45	-1	-11	>1000	>1000	>1000	88	87	77	1	
C1183	D1	52	-4	43	>1000	>1000	>1000	97	97	70	0	
C1301	D1	48	0	11	>1000	>1000	>1000	103	100	86	0.1	
C1647	D1	58	2	-23	>1000	>1000	>1000	86	91	89	2	
C2956	D1	53	-5	-1	>1000	>1000	>1000	102	116	99	1	
C5320	D1	42	-3	11	>1000	>1000	>1000	103	106	97	0.1	
C7765	D1	40	2	8	>1000	>1000	>1000	99	94	65	0.3	
C9077	D1	37	0	35	>1000	>1000	>1000	101	116	103	0	
10	D2	41	80	15	3	3	>200			55	2.7	>67
C0552	D2	-27	77	2	3	2	>100			41	0.5	>33
C0576	D2	-2	54	12	>1000	>1000	>1000	104	115	94	0.1	

Table S6. Continued.

		HTS (%)			IC_{50} (μM)[a]			% activity at 200 μM[b]			S.R.	
ID	**set**	***Ag*AChE1**	***Aa*AChE1**	***h*AChE[c]**	***Ag*AChE1**	***Aa*AChE1**	***h*AChE**	***Ag*AChE1**	***Aa*AChE1**	***h*AChE**	**HTS[d]**	**IC_{50}[e]**
C4073	D2	-5	80	40	n.d.	n.d.	n.d.				0	
C6303	D2	17	47	-16	>200	>200	>500	69	58	87	17	
C9270	D2	-40	69	15	n.d.	n.d.	n.d.				0.1	
1		93	91	99	0.26	0.44	0.030				0.9	0.07

[a]Compounds denoted n.d. could not be determined due to poor solubility. [b]If the IC_{50} value could not be determined from the used concentration range the enzyme activity at a compound concentration of 200 μM is given for comparison. [c]Previously published.[1] [d]If a compound inhibited an enzyme by ≤ 0% in a HTS the inhibition was set to 1% prior to calculation. The selectivity ratios were computed by taking the lower of the compound's inhibition (%) values against *Ag*AChE1 and *Aa*AChE1, and dividing by its inhibition (%) value against *h*AChE. [e]Selectivity ratios were computed by taking the compound's IC_{50} value against *h*AChE and dividing by the higher of its IC_{50} values against *Ag*AChE1 and *Aa*AChE1.

Dose-response analyses for IC_{50} determinations

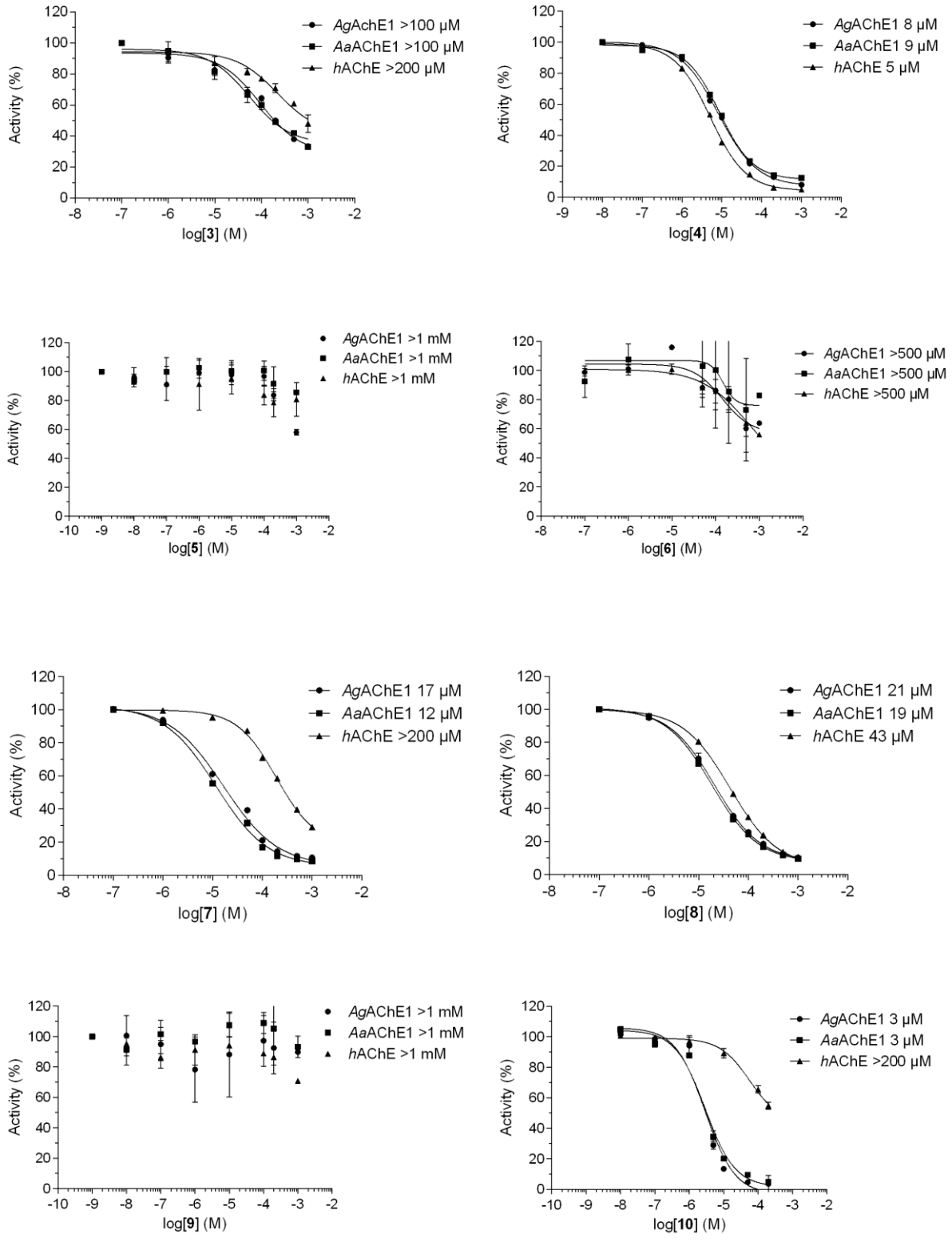

Figure S18. Graphs showing *IC_{50}*-determinations of compounds **3-10** in Table 2.

OPLS-DA model of AChE1- and *h*AChE selective hits

Table S7. Model statistics of the refined OPLS-DA model used to separate variation in the physicochemical properties related to the difference between the AChE1- and *h*AChE selective hits.

No of hits	157
No of descriptors	58
No of components	1+4
Eigenvalue of predictive component	8.89
Eigenvalue of last orthogonal component	3.71
R^2X (cum)	0.83
R^2Y (cum)	0.52
Q^2 (cum)	0.38

Table S8. Physicochemical descriptors included in the refined OPLS-DA model.

No.	Descriptor	Equal variance[a]	p-value[b]	No.	Descriptor	Equal variance[a]	p-value[b]
1	a_aro	no	0.0052	30	PEOE_PC-	yes	0.0033
2	a_heavy	yes	0.00017	31	PEOE_RPC+	yes	0.0027
3	a_IC	yes	0.026	32	PEOE_RPC-	no	4.6×10^{-5}
4	a_ICM	yes	6.0×10^{-5}	33	PEOE_VSA_FHYD	yes	7.3×10^{-6}
5	a_nC	yes	0.037	34	PEOE_VSA_FNEG	yes	0.00033
6	a_nH	yes	0.0011	35	PEOE_VSA_FPNEG	yes	0.00019
7	a_nO	yes	0.00019	36	PEOE_VSA_FPOL	yes	7.3×10^{-6}
8	a_nS	yes	0.028	37	PEOE_VSA_FPOS	yes	0.00033
9	bpol	yes	0.066	38	PEOE_VSA_FPPOS	yes	7.8x10-5
10	b_1rotN	yes	0.060	39	PEOE_VSA_NEG	yes	5.9×10^{-5}
11	b_1rotR	yes	0.00012	40	PEOE_VSA_PNEG	yes	0.00017
12	b_ar	no	0.0044	41	PEOE_VSA_POL	yes	1.3×10^{-5}
13	b_double	yes	3.0×10^{-8}	42	PEOE_VSA_PPOS	yes	9.6×10^{-5}
14	b_heavy	yes	0.00020	43	rings	yes	0.0027
15	b_max1len	yes	0.063	44	SlogP	yes	0.0024
16	b_rotR	yes	0.0023	45	SMR	yes	0.0032
17	b_single	yes	0.032	46	TPSA	yes	2.8×10^{-6}
18	chi0	yes	4.5×10^{-5}	47	VAdjEq	no	4.0×10^{-5}
19	chi0v	yes	0.0017	48	VAdjMa	no	8.2×10^{-5}
20	chi1	yes	0.00043	49	VDistMa	no	2.7×10^{-5}
21	chi1v	yes	0.032	50	vdw_area	yes	0.041
22	chi1_C	yes	0.041	51	vdw_vol	yes	0.033
23	density	yes	6.1×10^{-6}	52	vsa_acc	yes	6.5×10^{-5}
24	Kier1	yes	0.00022	53	vsa_other	yes	1.5×10^{-9}
25	KierA1	yes	0.066	54	vsa_pol	yes	0.00086
26	KierA3	no	0.011	55	Weight	yes	0.00016
27	KierFlex	yes	0.028	56	weinerPath	yes	0.021
28	logS	yes	3.2×10^{-13}	57	weinerPol	yes	3.0×10^{-6}
29	PEOE_PC+	yes	0.0033	58	zagreb	yes	3.6×10^{-5}

[a]According to F-test for sample variance based on the sets of *h*AChE- and the AChE1 selective hits in the model ($\alpha = 0.05$). [b]According to Student's T-test (two-tailed with $\alpha = 0.05$) assuming equal or unequal variance as decided by the F-test.

a)

b)

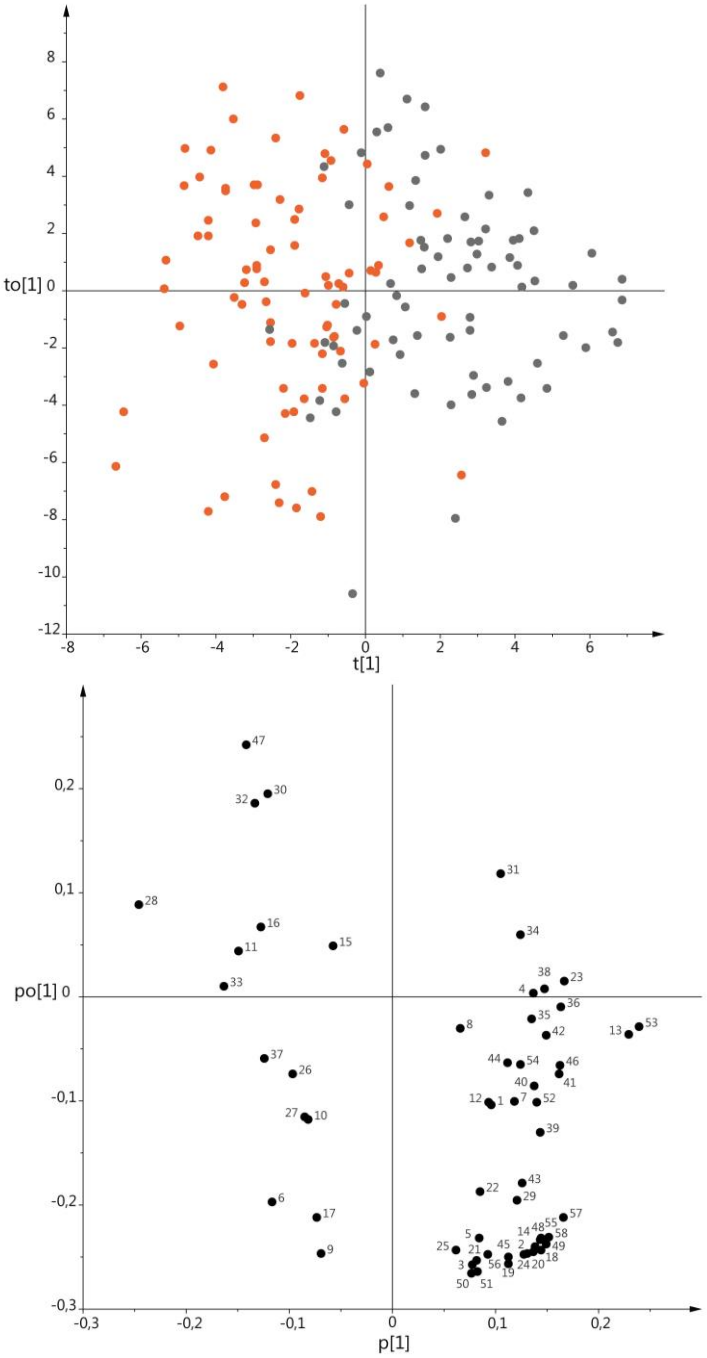

Figure S19. Score- and loading plot from the OPLS-DA model. a) Plot showing the score vectors of the predictive component (t[1]) vs. the first orthogonal component (to[1]). Hits showing potential selectivity for AChE1 and *h*AChE are shown as orange and grey dots, respectively. b) Plot showing the loading vectors of the predictive component (p[1]) vs. the first orthogonal component (po[1]). The predictive component mainly show separation due to size and flexibility.

NMR spectrum of compounds 3-10.

1-[3-(benzyloxy)-4-methoxybenzyl]-4-(4-fluorophenyl)-1,2,3,6-tetrahydropyridine (3). ^{1}H NMR (400 MHz, $(CD_3)_2SO$); LC-MS (ES) calcd for $C_{26}H_{27}FNO_2$ (M + H)+ 404, found 404

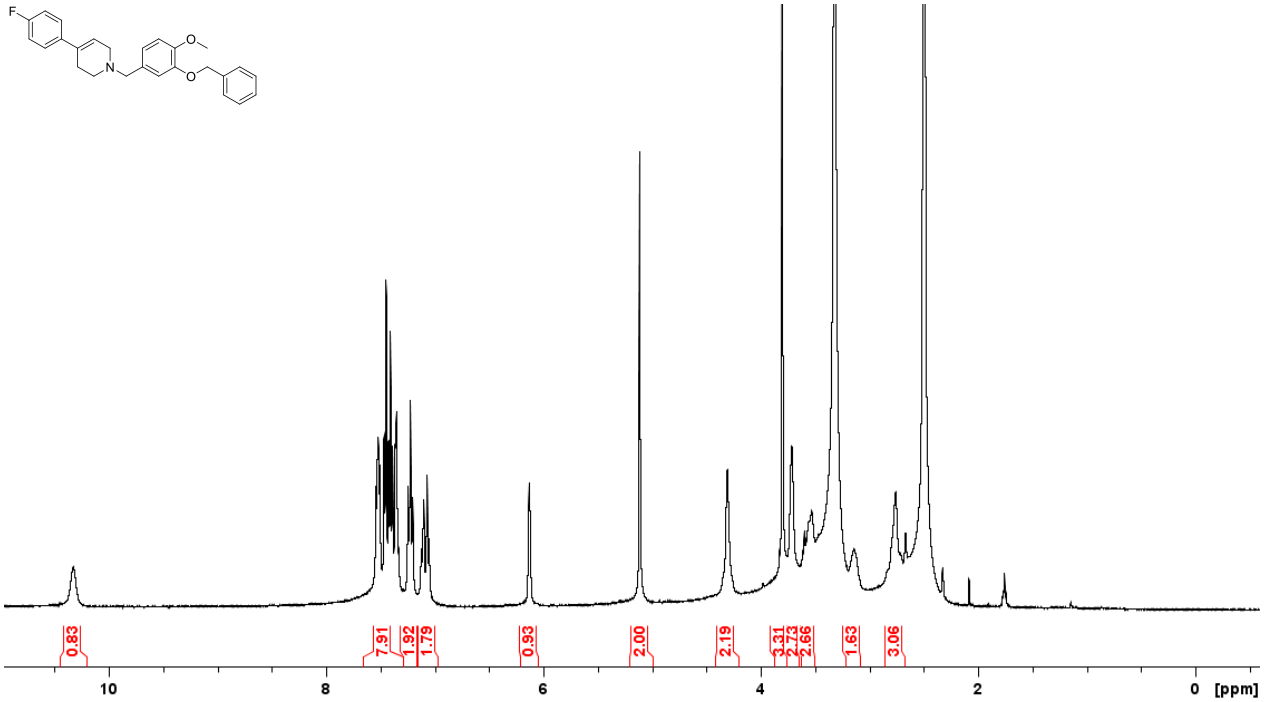

7-benzyl-2-(ethylthio)-3-phenyl-5,6,7,8-tetrahydropyrido[4',3':4,5]thieno[2,3-d]pyrimidin-4(3H)-one (4). ^{1}H NMR (400 MHz, $(CD_3)_2SO$); LC-MS (ES) calcd for $C_{24}H_{24}N_3OS_2$ (M + H)+ 435, found 435

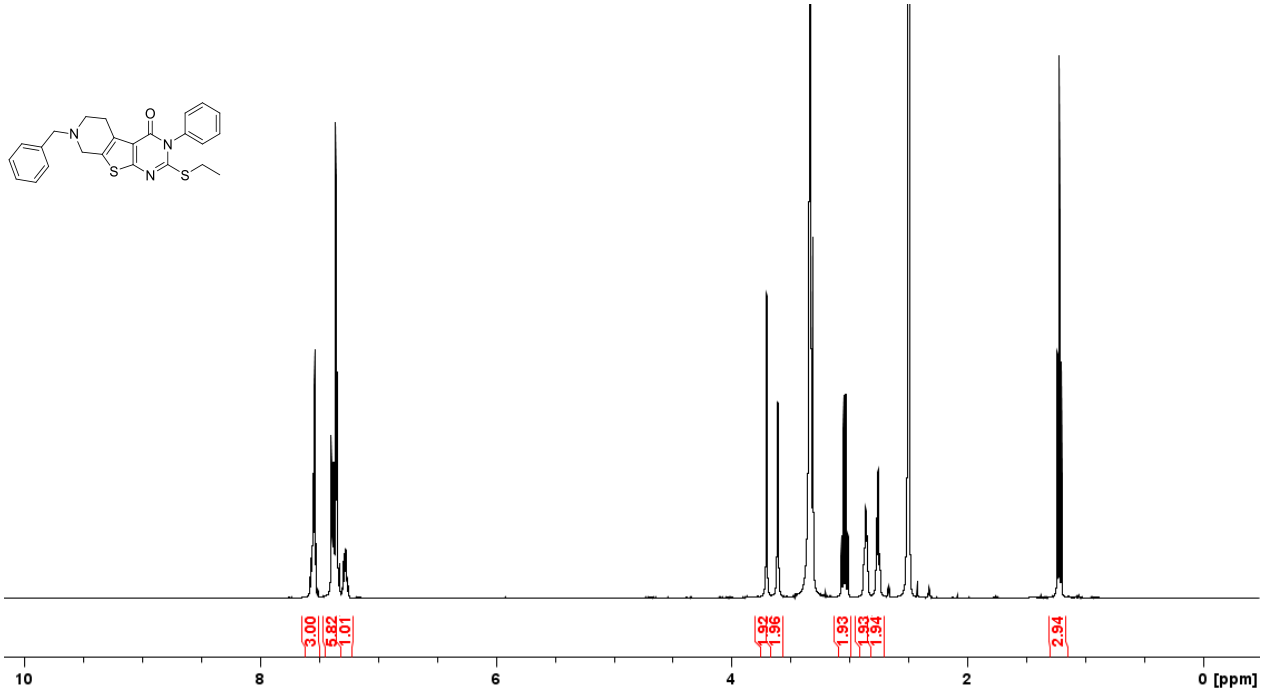

N-(2-{[5-(2-furyl)-4-phenyl-4H-1,2,4-triazol-3-yl]thio}ethyl)benzenesulfonamide (5). ^{1}H NMR (400 MHz, $(CD_3)_2SO$); LC-MS calcd for $C_{20}H_{19}N_4O_3S_2$ (M + H)+ 428, found 428

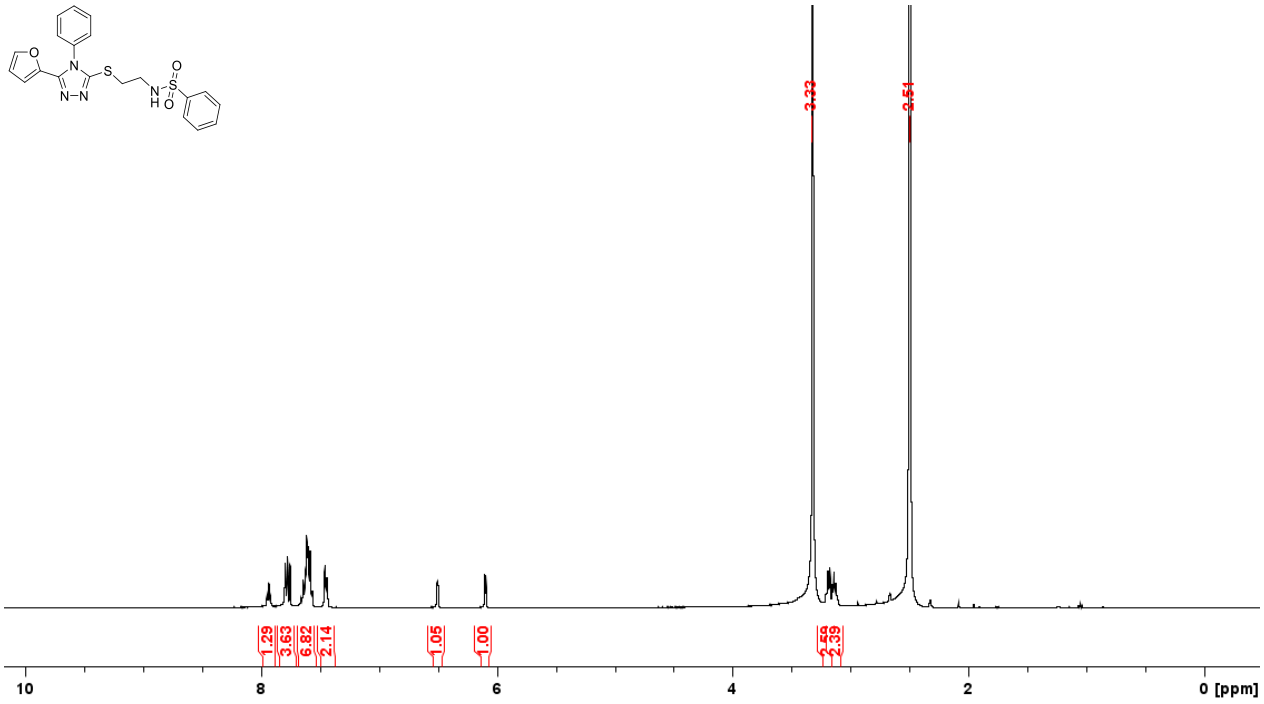

N-{2-[(2-fluorobenzyl)oxy]benzyl}-2-(4-morpholinyl)ethanamine dihydrochloride (6). ^{1}H NMR (400 MHz, $(CD_3)_2SO$); LC-MS calcd for $C_{20}H_{26}FN_2O_2$ (M + H)+ 345, found 345

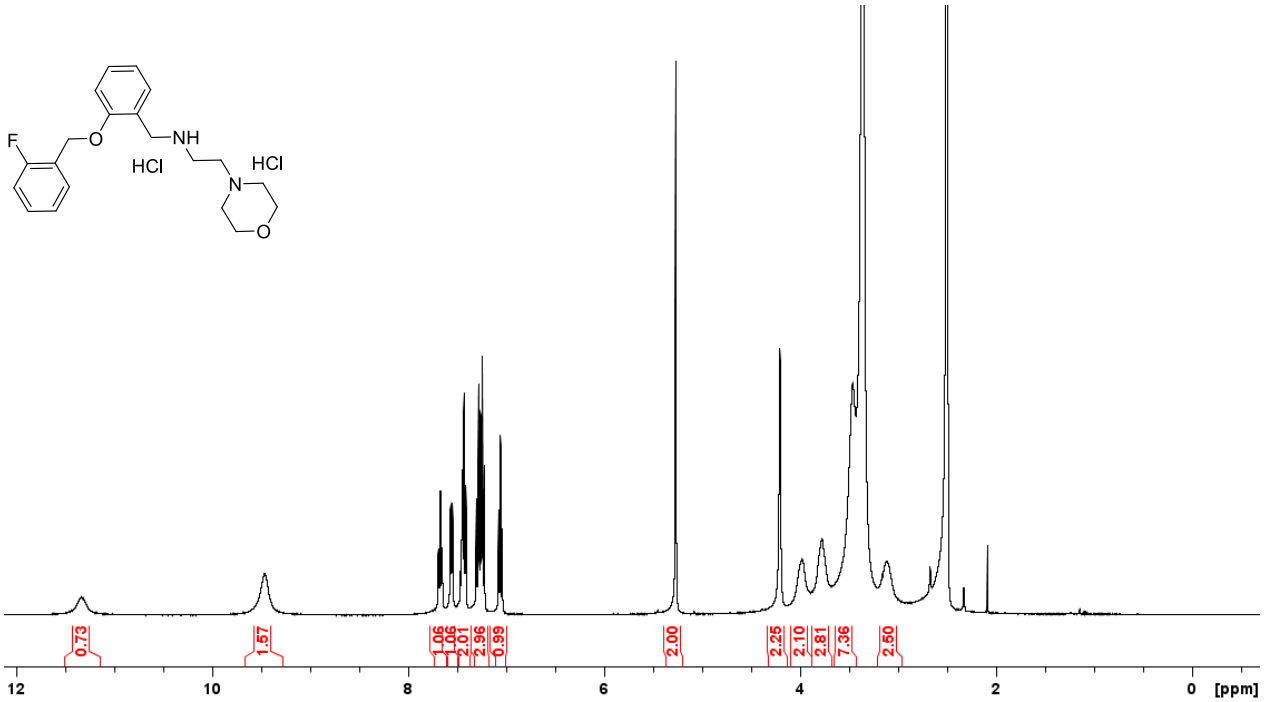

1-(1-benzyl-4-piperidinyl)-4-(2-fluorobenzoyl)piperazine (7). ^{1}H NMR (400 MHz, $(CD_3)_2SO$, 328 K); LC-MS calcd for $C_{23}H_{29}FN_3O$ (M + H)+ 382, found 382

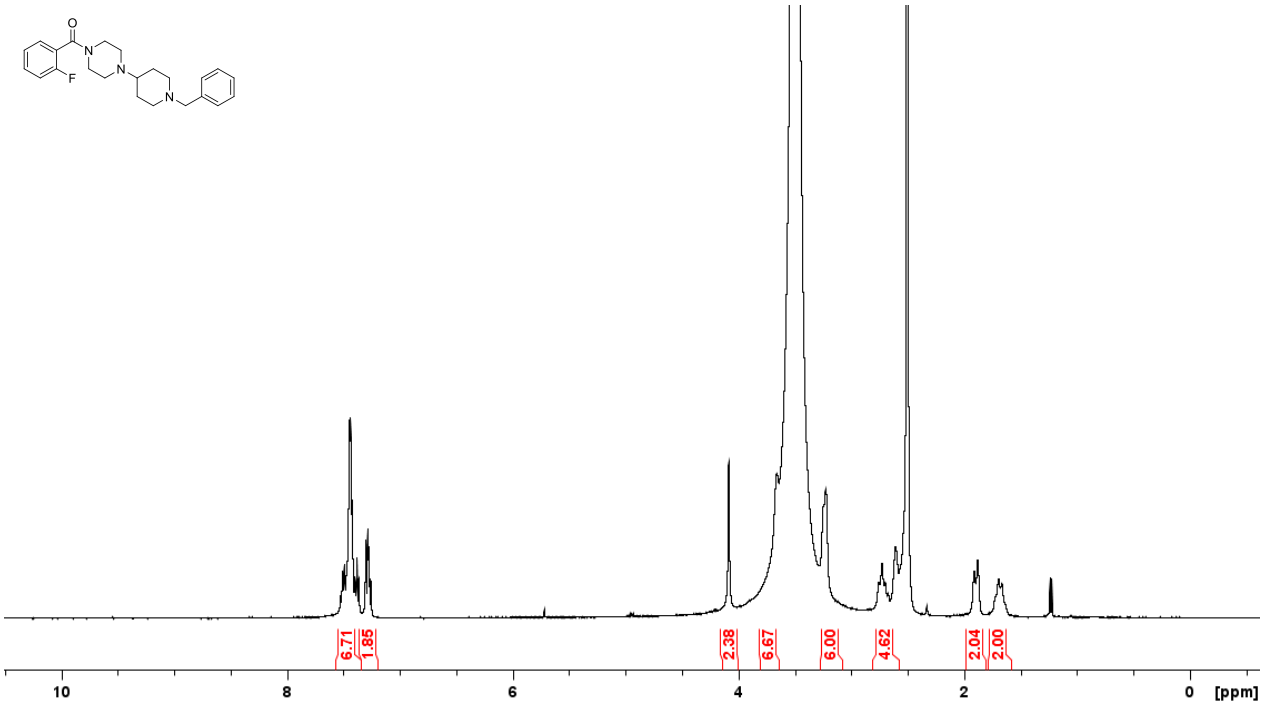

1-(1-benzyl-4-piperidinyl)-4-(phenoxyacetyl)piperazine (8). ^{1}H NMR (400 MHz, $(CD_3)_2SO$, 328 K); LC-MS calcd for $C_{24}H_{32}N_3O_2$ (M + H)+ 395, found 395

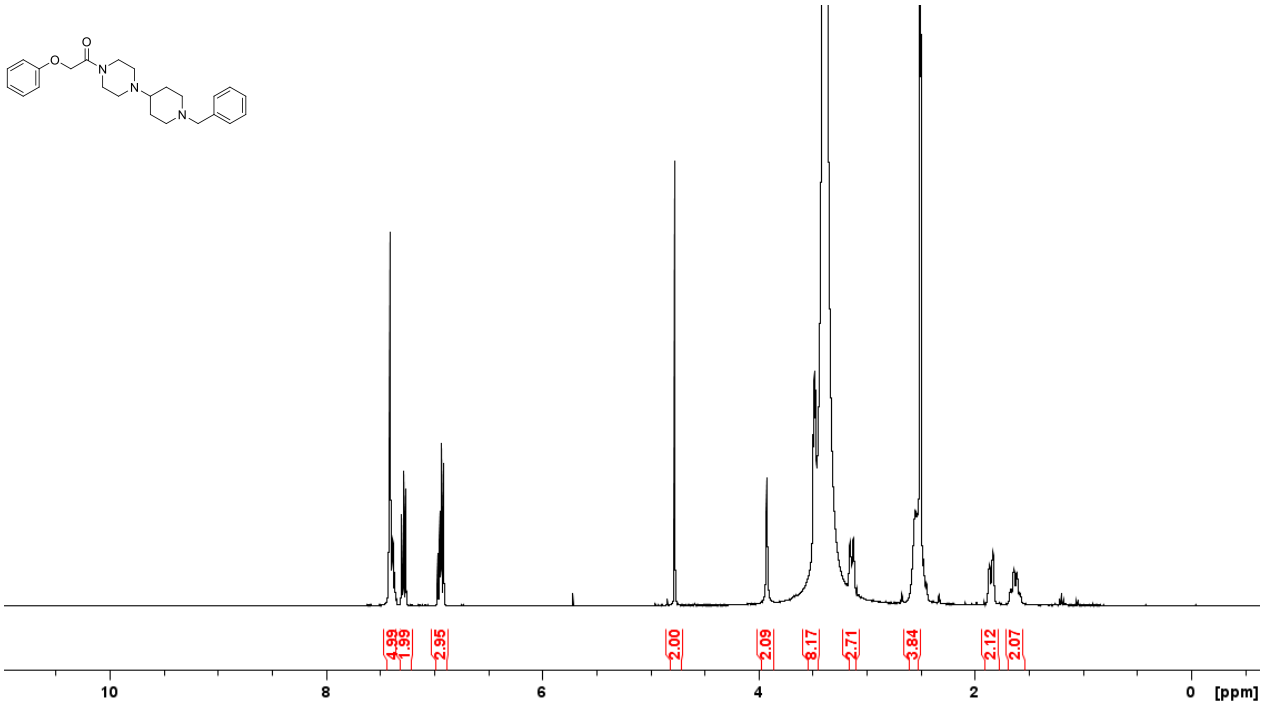

5-({[4-(4-ethoxyphenyl)-5-phenyl-4H-1,2,4-triazol-3-yl]thio}methyl)-3-(2-methylphenyl)-1,2,4-oxadiazole (9). ^{1}H NMR (400 MHz, $(CD_3)_2SO$); LC-MS calcd for $C_{26}H_{24}N_5O_2S$ (M + H)+ 471, found 471

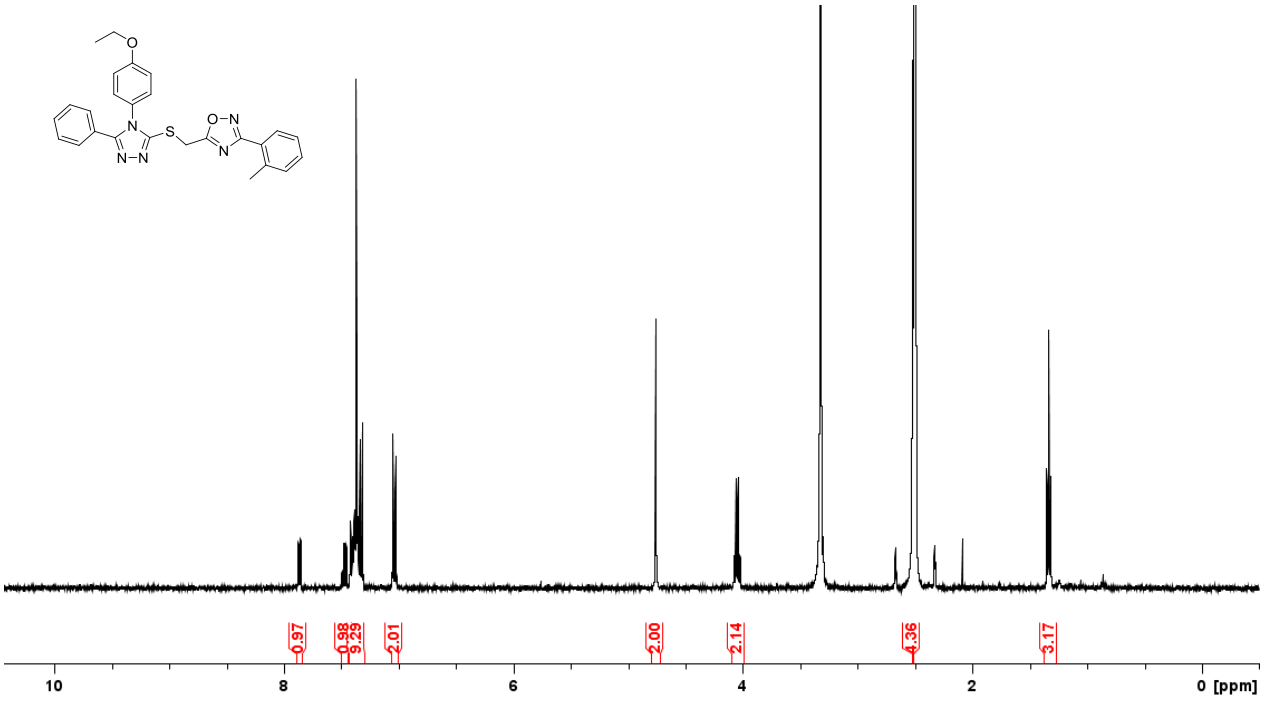

2-[4-(benzyloxy)benzyl]-1,2,3,4-tetrahydroisoquinoline (10). ^{1}H NMR (400 MHz, $(CD_3)_2SO$); LC-MS calcd for $C_{23}H_{24}NO$ (M + H)+ 330, found 330

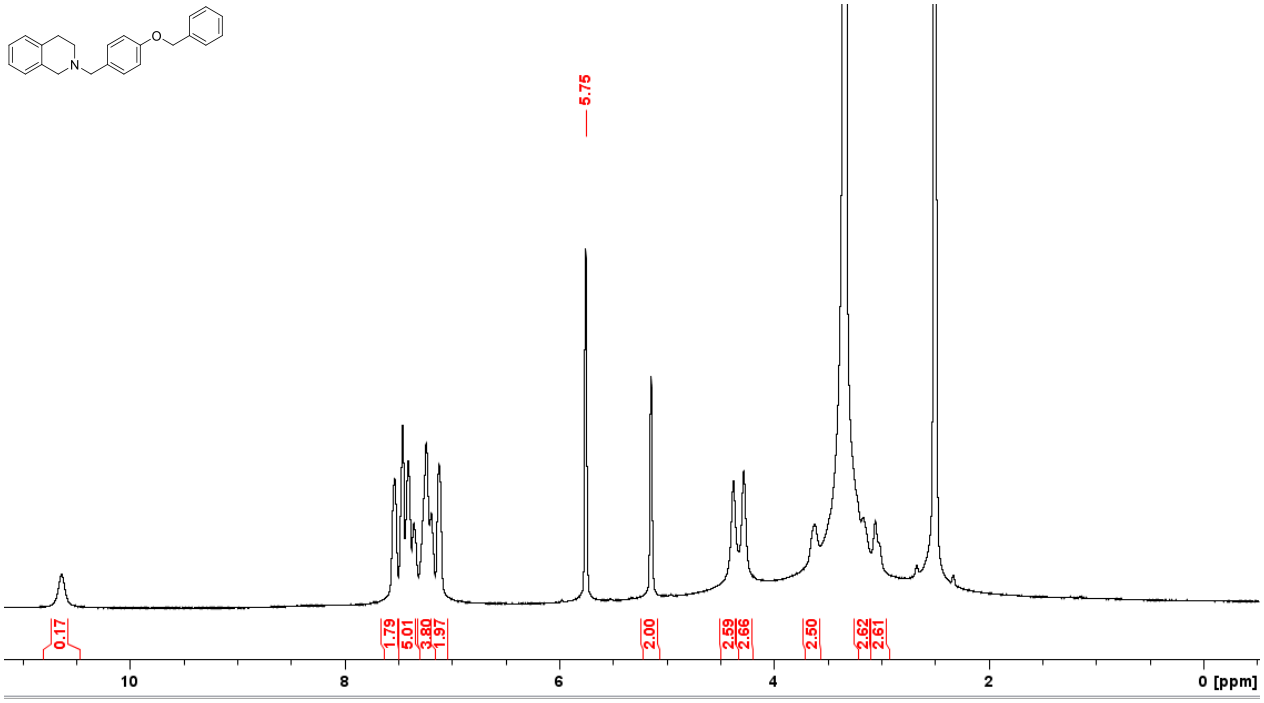

^{1}H and ^{13}C NMR spectrum of synthesized compounds

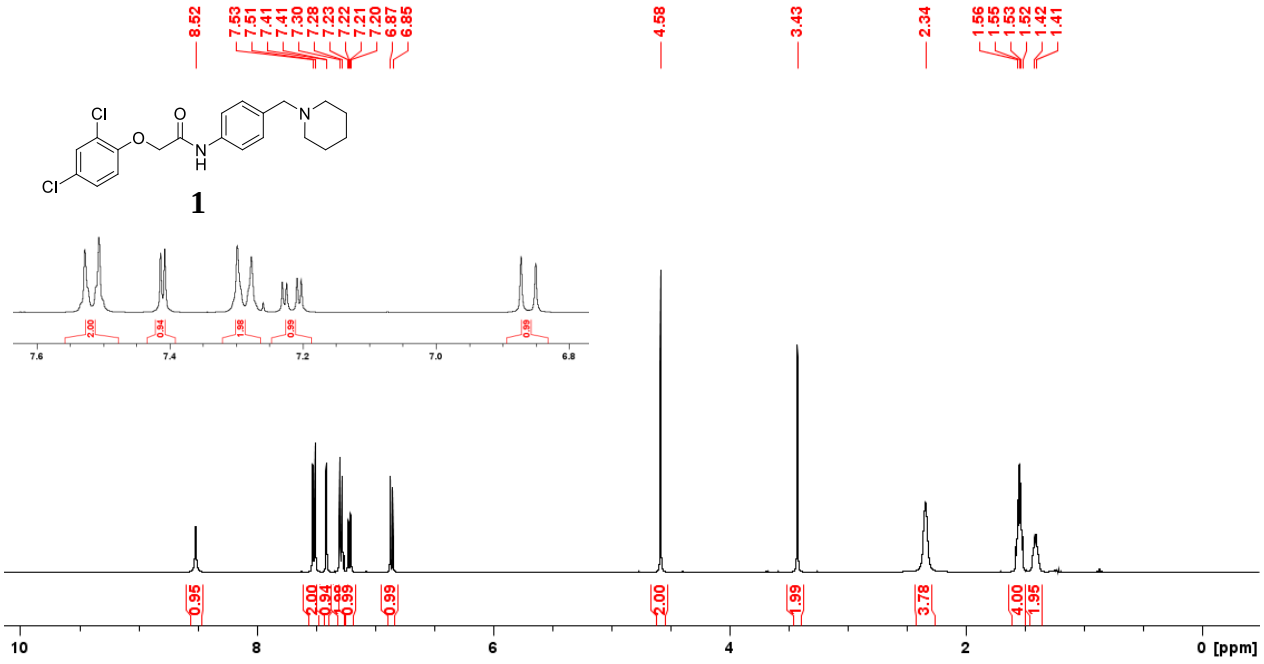

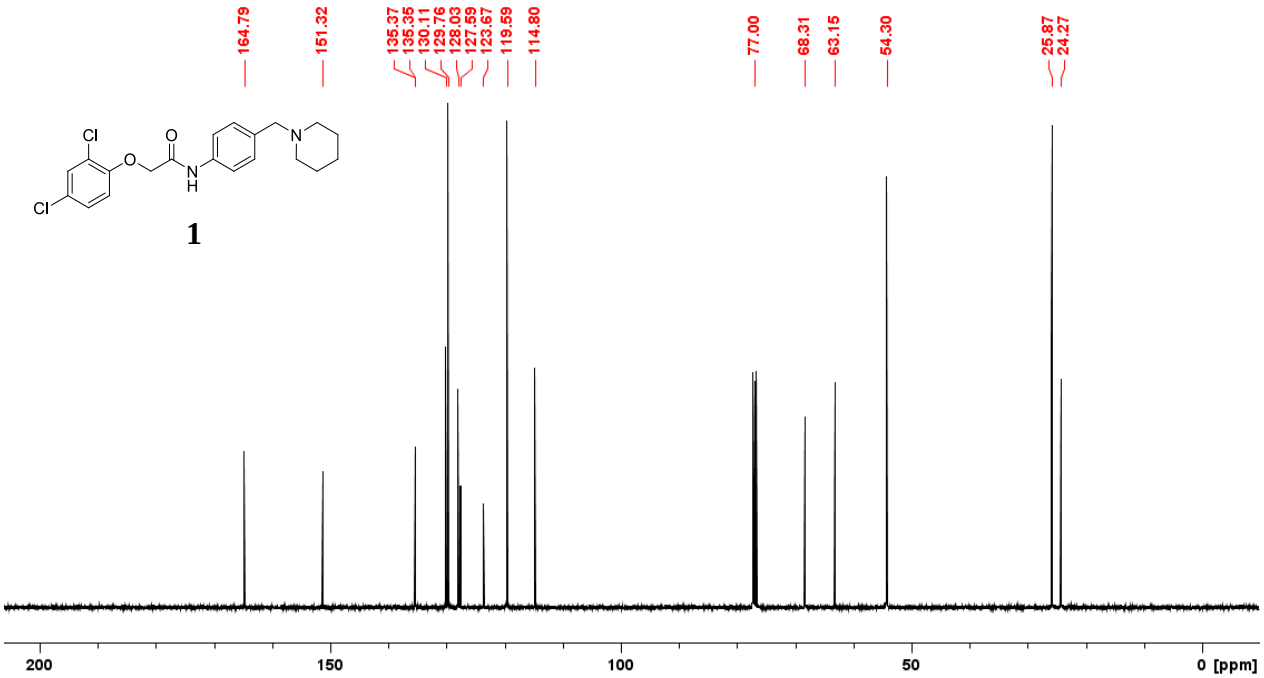

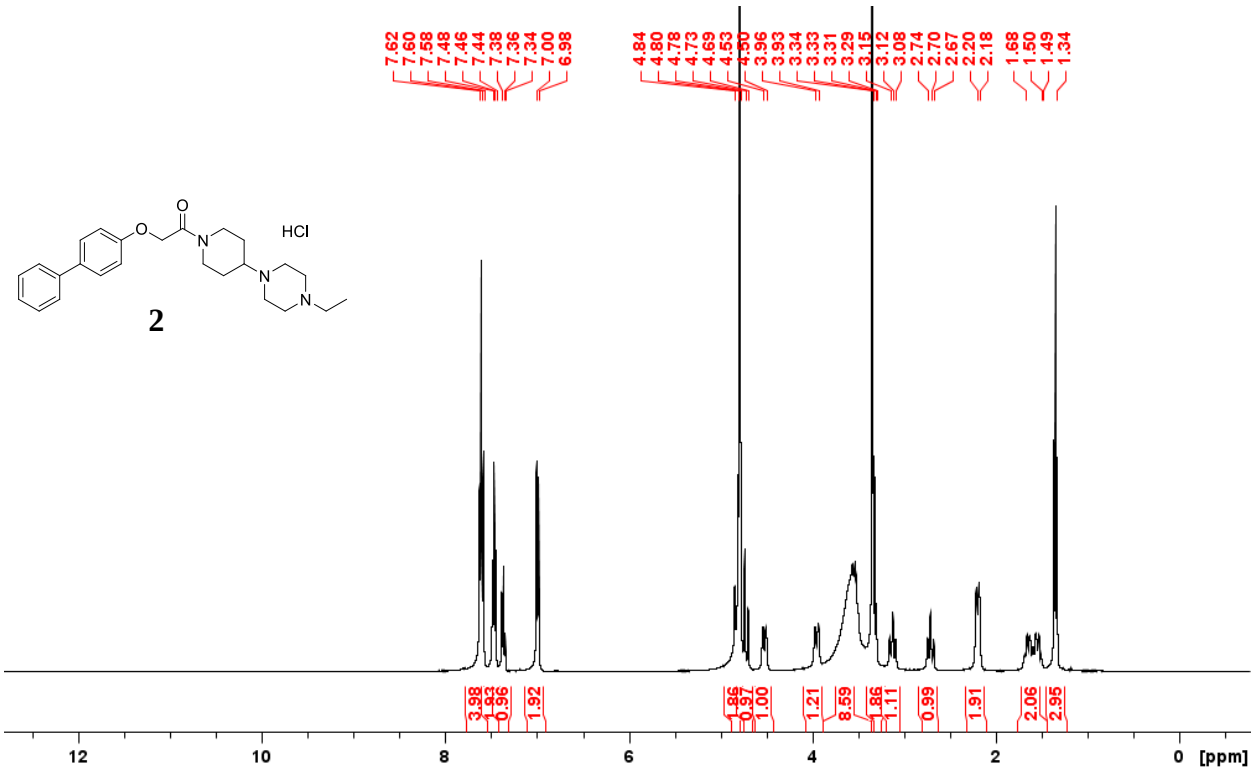
7.62
7.60
7.58
7.48
7.46
7.44
7.38
7.36
7.34
7.00
6.98
4.84
4.80
4.78
4.73
4.69
4.53
4.50
3.96
3.93
3.34
3.33
3.31
3.29
3.15
3.12
3.08
2.74
2.70
2.67
2.20
2.18
1.68
1.50
1.49
1.34
HCl
2
3.98
0.96
1.92
1.86
0.97
1.00
1.21
8.59
1.86
1.11
0.99
1.91
2.06
2.95
12
10
8
6
4
2
0
[ppm]

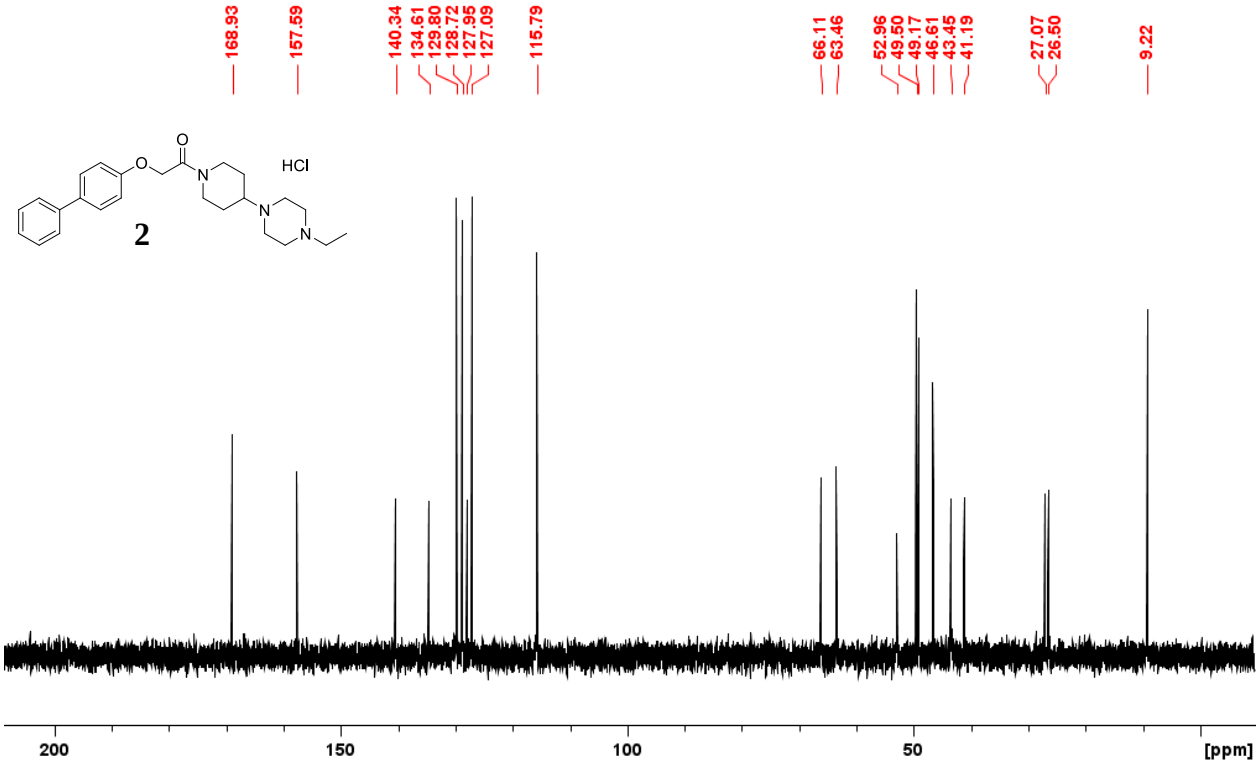
168.93
157.59
140.34
134.61
129.80
128.72
127.95
127.09
115.79
66.11
63.46
52.96
49.50
49.17
46.61
43.45
41.19
27.07
26.50
9.22
HCl
2
200
150
100
50
[ppm]

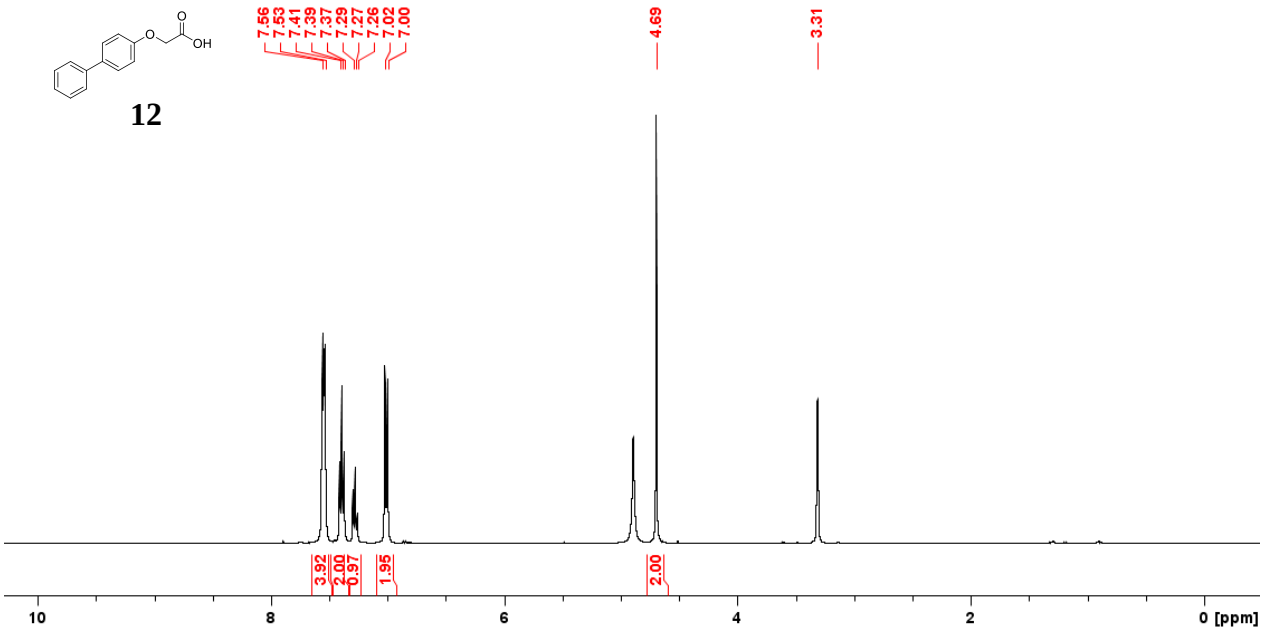
12
7.56
7.53
7.41
7.39
7.37
7.29
7.27
7.26
7.02
7.00
4.69
3.31
3.92
2.00
0.97
1.95
2.00
10
8
6
4
2
0 [ppm]

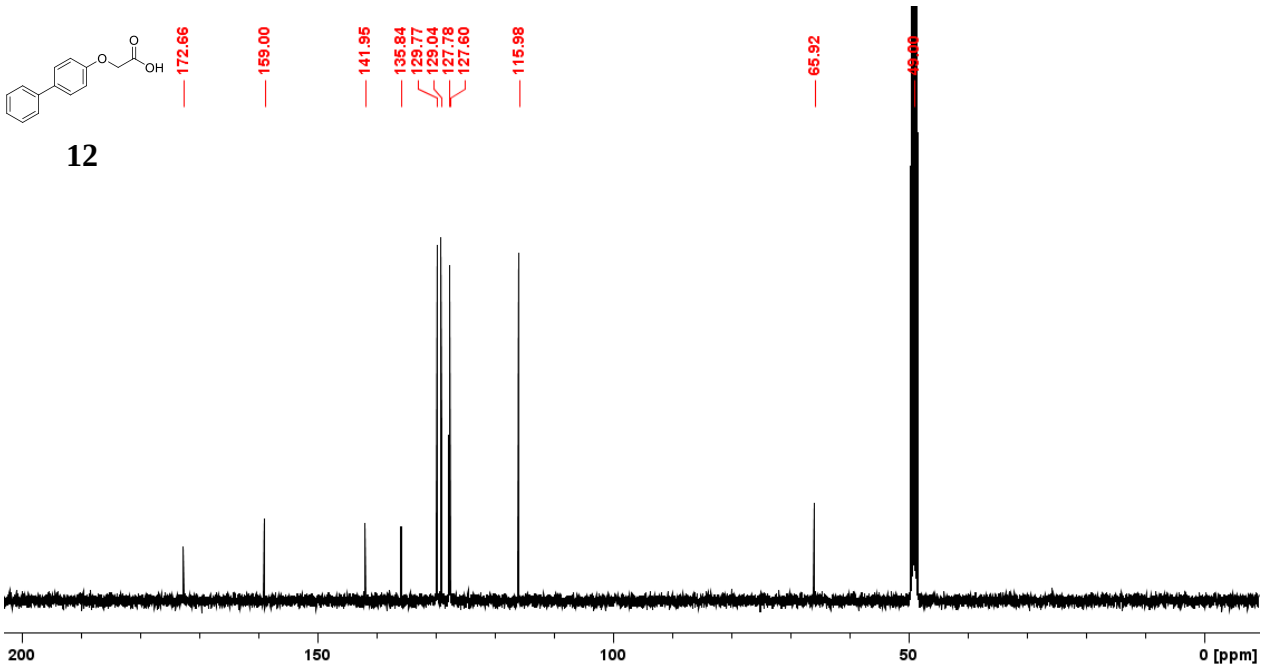
12
172.66
159.00
141.95
135.84
129.77
129.04
127.78
127.60
115.98
65.92
49.69
200
150
100
50
0 [ppm]

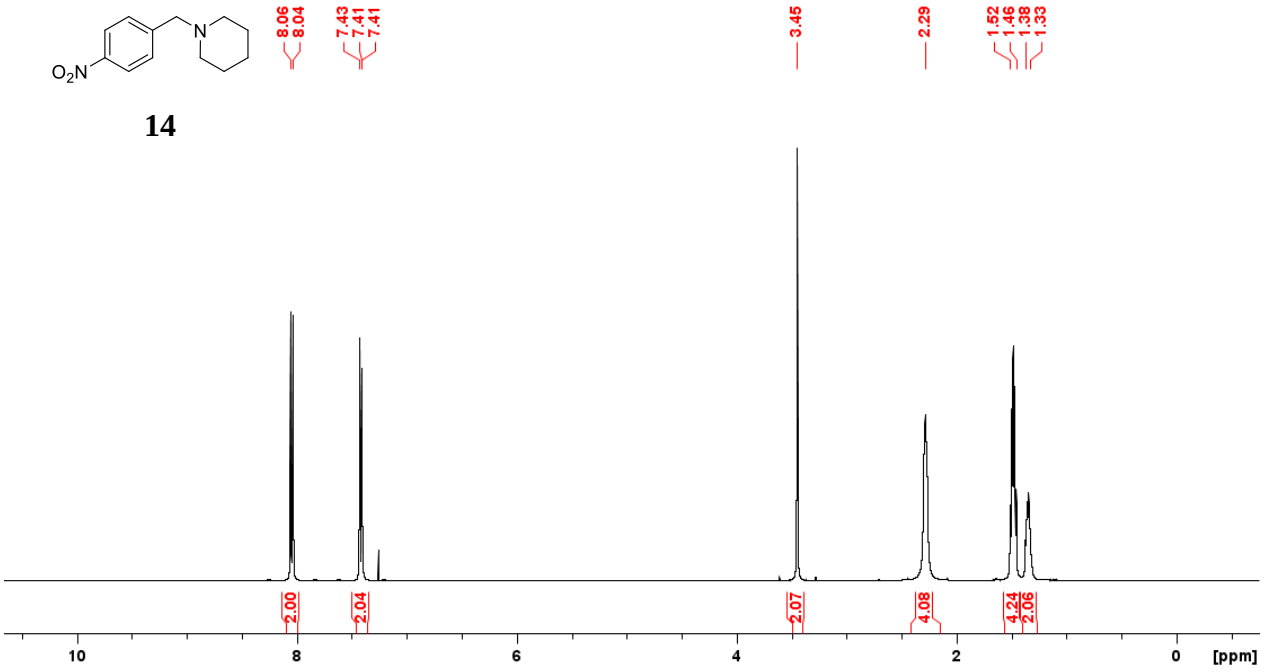
O2N
N
14
8.06
8.04
7.43
7.41
7.41
3.45
2.29
1.52
1.46
1.38
1.33
2.00
2.04
2.07
4.08
4.24
2.06
10
8
6
4
2
0
[ppm]

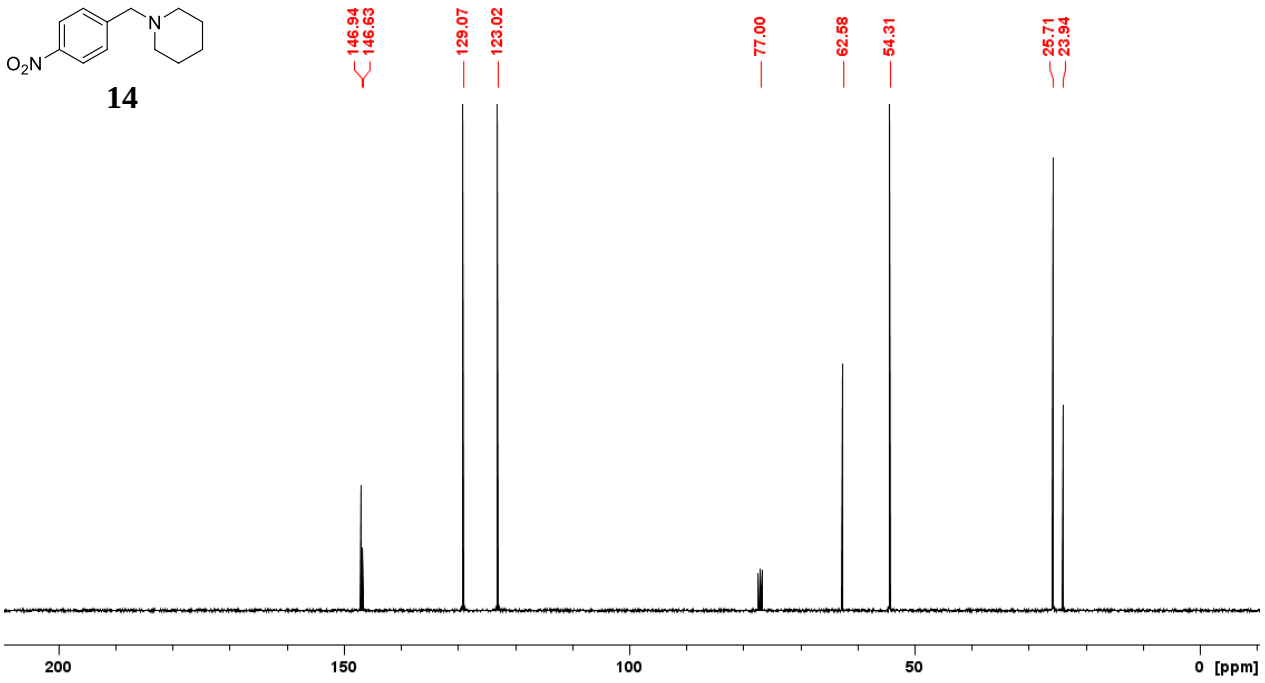
O2N
N
14
146.94
146.63
129.07
123.02
77.00
62.58
54.31
25.71
23.94
200
150
100
50
0
[ppm]

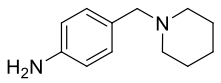
N
H2N

15

7.09
7.07
6.63
6.61
3.64
3.37
2.35
1.59
1.57
1.56
1.54
1.53
1.42
1.41
2.00
1.99
1.92
2.06
4.29
4.38
2.23
10
8
6
4
2
0
[ppm]

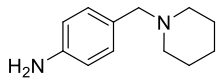
N
H2N

15

145.13
130.28
128.04
114.62
77.00
63.25
54.10
25.80
24.29
200
150
100
50
0 [ppm]

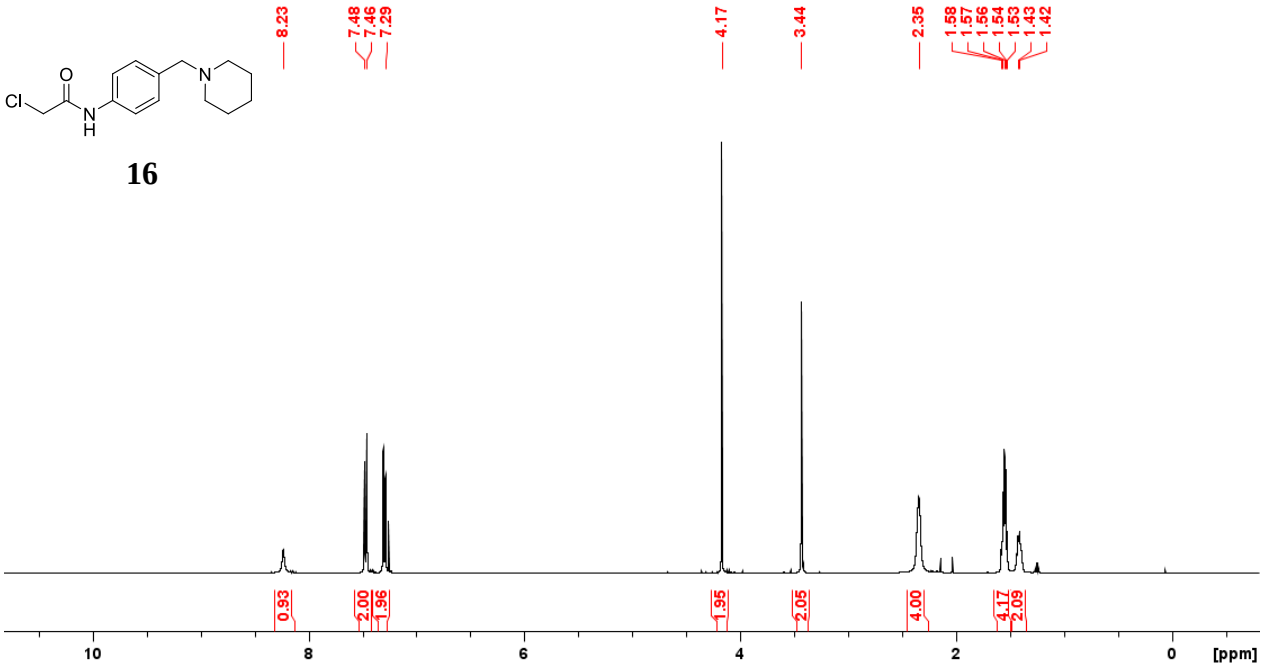
8.23
7.48
7.46
7.29
4.17
3.44
2.35
1.58
1.57
1.56
1.54
1.53
1.43
1.42
0.93
2.00
1.96
1.95
2.05
4.00
4.17
2.09
10
8
6
4
2
0
[ppm]

16

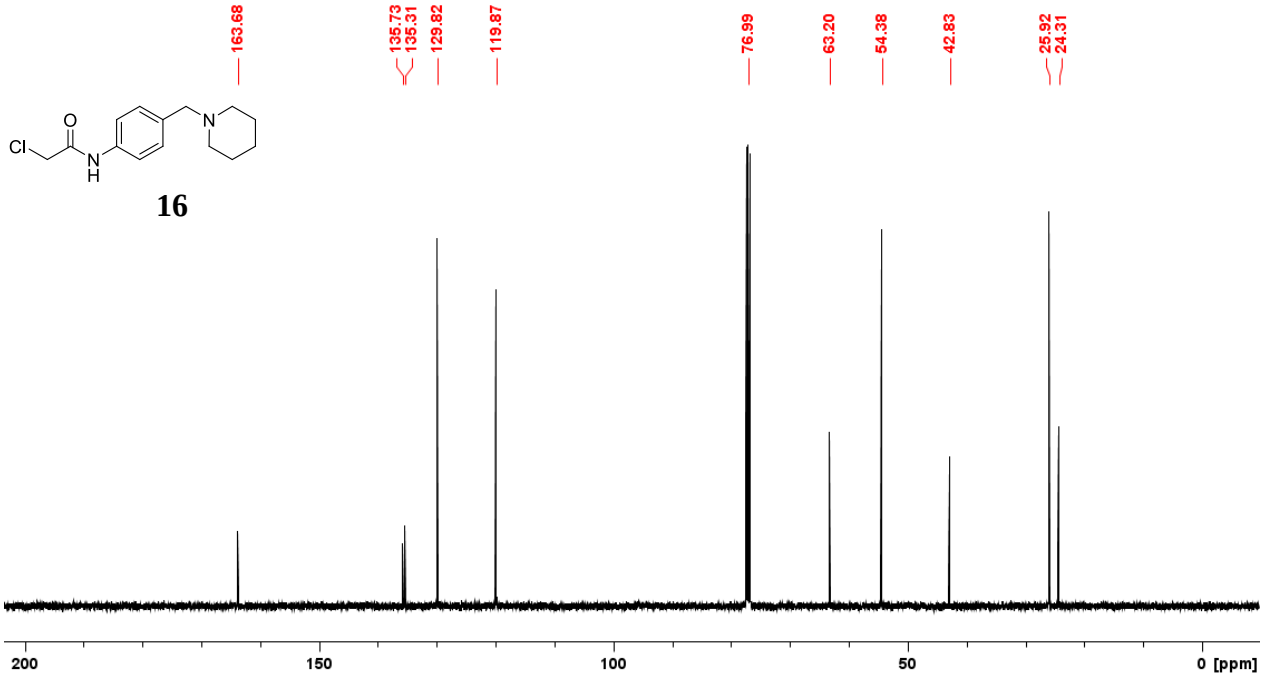
163.68
135.73
135.31
129.82
119.87
76.99
63.20
54.38
42.83
25.92
24.31
200
150
100
50
0 [ppm]

16

Multiple sequence alignment *Ag*AChE1

*Ag*AChE1 (accession no: XP_321792; UNIPROT code: ACES_ANOGA) after multiple alignment[3-4] with *Torpedo californica* (*Tc*AChE, PDB code: 1EA5, UNIPROT code: ACES_TORCA), *Homo sapiens* (*h*AChE, PDB code: 4EY4, UNIPROT code: ACES_HUMAN), *Mus musculus* (*m*AChE, PDB code: 1J06, UNIPROT code: ACES_MOUSE), and *Drosophila melanogaster* (*Dm*AChE, PDB code: 1QO9, UNIPROT code: ACES_DROME). Amino acids defined as 'loop one' and 'loop two' are highlighted in yellow and blue, respectively.

```
AgAChE1 DANDNDPLVVNTDKGRIRGITVDAPSGKKVDVWLGIPYAQPPVGPLRFRHPRPAEK-WTG
hAChE   EGREDAELLVTVRGGRLRGIRLKTPGG-PVSAFLGIPFAEPPMGPRRFLPPEP-KQPWSG
mAChE   EGREDPQLLVRVRGGQLRGIRLKAPGG-PVSAFLGIPFAEPPVGSRRFMPPEP-KRPWSG
DmAChE  VCGVIDRLVVQTSSGPVRGRSVTVQG-REVHVYTGIPYAKPPVEDLRFRKPVPAE-PWHG
TcAChE  QADDHSELLVNTKSGKVMGTRVPVLSS-HISAFLGIPFAEPPVGNMRFRRPEP-KKPWSG

AgAChE1 VLNTTTPPNSCVQIVDTVFGDFPGATMWNPNTPLSEDCLYINVVAPRPRPKNAA-VMLWI
hAChE   VVDATTFQSVCYQYVDTLYPGFEGTEMWNPNRELSEDCLYLNVWTPYPRPTSPTPVLVWI
mAChE   VLDATTFQNVCYQYVDTLYPGFEGTEMWNPNRELSEDCLYLNVWTPYPRPASPTPVLIWI
DmAChE  VLDATGLSATCVQERYEYFPGFSGEEIWNPNTNVSEDCLYINVWAPAKNTTNGLPILIWI
TcAChE  VWNASTYPNNCQQYVDEQFPGFSGSEMWNPNREMSEDCLYLNIWVPSPRPKSTT-VMVWI

AgAChE1 FGGGFYSGTATLDVYDHRALAS-EENVIVVSLQYRVASLGFLFL-------GTPEAPGNA
hAChE   YGGGFYSGASSLDVYDGRFLVQAE-RTVLVSMNYRVGAFGFLALP------GSREAPGNV
mAChE   YGGGFYSGAASLDVYDGRFLAQVEGA-VLVSMNYRVGTFGFLALP------GSREAPGNV
DmAChE  YGGGFMTGSATLDIYNADIMAAV-GNVIVASFQYRVGAFGFLHLAPEMPSEFAEEAPGNV
TcAChE  YGGGFYSGSSTLDVYNGKYLAYTEE-VVLVSLSYRVGAFGFLALH------GSQEAPGNV

AgAChE1 GLFDQNLALRWVRDNIHRFGGDPSRVTLFGESAGAVSVSLHLLSALSRDLFQRAILQSGS
hAChE   GLLDQRLALQWVQENVAAFGGDPTSVTLFGESAGAASVGMHLLSPPSRGLFHRAVLQSGA
mAChE   GLLDQRLALQWVQENIAAFGGDPMSVTLFGESAGAASVGMHILSLPSRSLFHRAVLQSGT
DmAChE  GLWDQALAIRWLKDNAHAFGGNPEWMTLFGESAGSSSVNAQLMSPVTRGLVKRGMMQSGT
TcAChE  GLLDQRMALQWVHDNIQFFGGDPKTVTIFGESAGGASVGMHILSPGSRDLFRRAILQSGS

AgAChE1 PTAPWALVSREEATLR-ALRLAEAVGCP--HEPSKLSDAVECLRGKDP-HVLVNNEWGTL
hAChE   PNGPWATVGMGEARRR-ATQLAHLVGCPPGGTGGNDTELVACLRTR-PAQVLVNHEWHVL
mAChE   PNGPWATVSAGEARRR-ATLLARLVGCPPGGAGGNDTELIACLRTR-PAQDLVDHEWHVL
DmAChE  MNAPWSHMTSEKAVEIGKALINDC-NCNASMLKTNPAHVMSCMRSVD-AKTISVQQWNSY
TcAChE  PNCPWASVSVAEGRRR-AVELGRNLNCN----LNSDEELIHCLREKKP-QELIDVEWNVL

AgAChE1 G---ICEFPFVPVVDGAFLDETPQRSLASGRFKKTEILTGSNTEEGYYFIIYYLTELLRK
hAChE   PQESVFRFSFVPVVDGDFLSDTPEALINAGDFHGLQVLVGVVKDEGSYFLVY-GAPGFSK
mAChE   PQESIFRFSFVPVVDGDFLSDTPEALINTGDFQDLQVLVGVVKDEGSYFLVY-GVPGFSK
DmAChE  S--GILSFPSAPTIDGAFLPADPMTLMKTADLKDYDILMGNVRDEGTYFLLYDFIDYFDK
TcAChE  PFDSIFRFSFVPVIDGEFFPTSLESMLNSGNFKKTQILLGVNKDEGSFFLLY-GAPGFSK

AgAChE1 EEGVTVTREEFLQAVRELNPYVNGAARQAIVFEYTDWTEPDNPNSNRDALDKMVGDYHFT
hAChE   DNESLISRAEFLAGVRVGVPQVSDLAAEAVVLHYTDWLHPEDPARLREALSDVVGDHNVV
mAChE   DNESLISRAQFLAGVRIGVPQASDLAAEAVVLHYTDWLHPEDPTHLRDAMSAVVGDHNVV
DmAChE  DDATALPRDKYLEIMNNIFGKATQAEREAIIFQYTSWEG-NPGYQNQQQIGRAVGDHFFT
TcAChE  DSESKISREDFMSGVKLSVPHANDLGLDAVTLQYTDWMDDNNGIKNRDGLDDIVGDHNVI

AgAChE1 CNVNEFAQRYAEEGNNVYMYLYTHRSKGNPWPRWTGVMHGDEINYVFGEPLNPTLGYTED
hAChE   CPVAQLAGRLAAQGARVYAYVFEHRASTLSWPLWMGVPHGYEIEFIFGIPLDPSRNYTAE
mAChE   CPVAQLAGRLAAQGARVYAYIFEHRASTLTWPLWMGVPHGYEIEFIFGLPLDPSLNYTTE
DmAChE  CPTNEYAQALAERGASVHYYYFTHRTSTSLWGEWMGVLHGDEIEYFFGQPLNNSLQYRPV
TcAChE  CPLMHFVNKYTKFGNGTYLYFFNHRASNLVWPEWMGVIHGYEIEFVFGLPLVKELNYTAE

AgAChE1 EKDFSRKIMRYWSNFAKTGNPNPNTASSEFPEWPKHTAHGRHYLELGL--NTSFVGRGPR
hAChE   EKIFAQRLMRYWANFARTGDPN-EPRDPKAPQWPPYTAGAQQYVSLDL--RPLEVRRGLR
mAChE   ERIFAQRLMKYWTNFARTGDPN-DPRDSKSPQWPPYTTAAQQYVSLNL--KPLEVRRGLR
DmAChE  ERELGKRMLSAVIEFAKTGNPAQD-----GEEWPNFSKEDPVYYIFSTDDKIEKLARGPL
TcAChE  EEALSRRIMHYWATFAKTGNPN-EPHSQESK-WPLFTTKEQKFIDLNT--EPMKVHQRLR

AgAChE1 LRQCAFWKKYLPQLVAAT
hAChE   AQACAFWNRFLPKLLSAT
mAChE   AQTCAFWNRFLPKLLSAT
DmAChE  AARCSFWNDYLPKVRSWA
TcAChE  VQMCVFWNQFLPKLLNAT
```

Multiple sequence alignment *Aa*AChE1

*Aa*AChE1 (accession no: ABN09910) after multiple alignment[3-4] with *Torpedo californica* (*Tc*AChE, PDB code: 1EA5, UNIPROT code: ACES_TORCA), *Homo sapiens* (*h*AChE, PDB code: 4EY4, UNIPROT code: ACES_HUMAN), *Mus musculus* (*m*AChE, PDB code: 1J06, UNIPROT code: ACES_MOUSE), and *Drosophila melanogaster* (*Dm*AChE, PDB code: 1QO9, UNIPROT code: ACES_DROME). Amino acids defined as 'loop one' and 'loop two' are highlighted in yellow and blue, respectively.

```
AaAChE1 DGTDNDPLLITTDKGKVRGLTLEAPSGKKVDAWLGIPYAQPPLGPLRFRHPRPVEK-WTG
hAChE   EGREDAELLVTVRGGRLRGIRLKTPGG-PVSAFLGIPFAEPPMGPRRFLPPEP-KQPWSG
mAChE   EGREDPQLLVRVRGGQLRGIRLKAPGG-PVSAFLGIPFAEPPVGSRRFMPPEP-KRPWSG
DmAChE  VCGVIDRLVVQTSSGPVRGRSVTVQG-REVHVYTGIPYAKPPVEDLRFRKPVPAE-PWHG
TcAChE  QADDHSELLVNTKSGKVMGTRVPVLSS-HISAFLGIPFAEPPVGNMRFRRPEP-KKPWSG

AaAChE1 VLNATTPPNSCVQIVDTVFGDFPGATMWNPNTPLSEDCLYINVVVPHPRPKNSA-VMLWI
hAChE   VVDATTFQSVCYQYVDTLYPGFEGTEMWNPNRELSEDCLYLNVWTPYPRPTSPTPVLVWI
mAChE   VLDATTFQNVCYQYVDTLYPGFEGTEMWNPNRELSEDCLYLNVWTPYPRPASPTPVLIWI
DmAChE  VLDATGLSATCVQERYEYFPGFSGEEIWNPNTNVSEDCLYINVWAPAKNTTNGLPILIWI
TcAChE  VWNASTYPNNCQQYVDEQFPGFSGSEMWNPNREMSEDCLYLNIWVPSPRPKSTT-VMVWI

AaAChE1 FGGGFYSGTATLDVYDHRTLAS-EENVIVVSLQYRVASLGFLFL-------GTPEAPGNA
hAChE   YGGGFYSGASSLDVYDGRFLVQAE-RTVLVSMNYRVGAFGFLALP------GSREAPGNV
mAChE   YGGGFYSGAASLDVYDGRFLAQVEGA-VLVSMNYRVGTFGFLALP------GSREAPGNV
DmAChE  YGGGFMTGSATLDIYNADIMAAV-GNVIVASFQYRVGAFGFLHLAPEMPSEFAEEAPGNV
TcAChE  YGGGFYSGSSTLDVYNGKYLAYTEE-VVLVSLSYRVGAFGFLALH------GSQEAPGNV

AaAChE1 GLFDQNLALRWVRDNIHKFGGDPSRVTLFGESAGAVSVSLHLLSALSRDLFQRAILQSGS
hAChE   GLLDQRLALQWVQENVAAFGGDPTSVTLFGESAGAASVGMHLLSPPSRGLFHRAVLQSGA
mAChE   GLLDQRLALQWVQENIAAFGGDPMSVTLFGESAGAASVGMHILSLPSRSLFHRAVLQSGT
DmAChE  GLWDQALAIRWLKDNAHAFGGNPEWMTLFGESAGSSSVNAQLMSPVTRGLVKRGMMQSGT
TcAChE  GLLDQRMALQWVHDNIQFFGGDPKTVTIFGESAGGASVGMHILSPGSRDLFRRAILQSGS

AaAChE1 PTAPWALVSREEATLR-ALRLAEAVNCP--HDATKLTDTVECLRTKDP-NVLVDNEWGTL
hAChE   PNGPWATVGMGEARRR-ATQLAHLVGCPPGGTGGNDTELVACLRTR-PAQVLVNHEWHVL
mAChE   PNGPWATVSAGEARRR-ATLLARLVGCPPGGAGGNDTELIACLRTR-PAQDLVDHEWHVL
DmAChE  MNAPWSHMTSEKAVEIGKALINDC-NCNASMLKTNPAHVMSCMRSVD-AKTISVQQWNSY
TcAChE  PNCPWASVSVAEGRRR-AVELGRNLNCN----LNSDEELIHCLREKKP-QELIDVEWNVL

AaAChE1 G---ICEFPFVPVVDGAFLDETPQRSLASGRFKKTDILTGSNTEEGYYFIIYYLTELLRK
hAChE   PQESVFRFSFVPVVDGDFLSDTPEALINAGDFHGLQVLVGVVKDEGSYFLVY-GAPGFSK
mAChE   PQESIFRFSFVPVVDGDFLSDTPEALINTGDFQDLQVLVGVVKDEGSYFLVY-GVPGFSK
DmAChE  S--GILSFPSAPTIDGAFLPADPMTLMKTADLKDYDILMGNVRDEGTYFLLYDFIDYFDK
TcAChE  PFDSIFRFSFVPVIDGEFFPTSLESMLNSGNFKKTQILLGVNKDEGSFFLLY-GAPGFSK

AaAChE1 EEGVTVSREEFLQAVRELNPYVVNGAARQAIVFEYTDWTEPENPNSNRDALDKMVGDYHFT
hAChE   DNESLISRAEFLAGVRVGVPQVSDLAAEAVVLHYTDWLHPEDPARLREALSDVVGDHNVV
mAChE   DNESLISRAQFLAGVRIGVPQASDLAAEAVVLHYTDWLHPEDPTHLRDAMSAVVGDHNVV
DmAChE  DDATALPRDKYLEIMNNIFGKATQAEREAIIFQYTSWEG-NPGYQNQQQIGRAVGDHFFT
TcAChE  DSESKISREDFMSGVKLSVPHANDLGLDAVTLQYTDWMDDNNGIKNRDGLDDIVGDHNVI

AaAChE1 CNVNEFAQRYAEEGNNVYMYLYTHRSKGNPWPRWTGVMHGDEINYVFGEPLNSDLGYMED
hAChE   CPVAQLAGRLAAQGARVYAYVFEHRASTLSWPLWMGVPHGYEIEFIFGIPLDPSRNYTAE
mAChE   CPVAQLAGRLAAQGARVYAYIFEHRASTLTWPLWMGVPHGYEIEFIFGLPLDPSLNYTTE
DmAChE  CPTNEYAQALAERGASVHYYYFTHRTSTSLWGEWMGVLHGDEIEYFFGQPLNNSLQYRPV
TcAChE  CPLMHFVNKYTKFGNGTYLYFFNHRASNLVWPEWMGVIHGYEIEFVFGLPLVKELNYTAE

AaAChE1 EKDFSRKIMRYWSNFAKTGNPNPSPPNSDFPEWPKHTAHGRHYLELGL--NTTYVGRGPR
hAChE   EKIFAQRLMRYWANFARTGDPN-EPRDPKAPQWPPYTAGAQQYVSLDL--RPLEVRRGLR
mAChE   ERIFAQRLMKYWTNFARTGDPN-DPRDSKSPQWPPYTTAAQQYVSLNL--KPLEVRRGLR
DmAChE  ERELGKRMLSAVIEFAKTGNPAQD-----GEEWPNFSKEDPVYYIFSTDDKIEKLARGPL
TcAChE  EEALSRRIMHYWATFAKTGNPN-EPHSQESK-WPLFTTKEQKFIDLNT--EPMKVHQRLR

AaAChE1 LRQCAFWKKYLPQLVAAT
hAChE   AQACAFWNRFLPKLLSAT
mAChE   AQTCAFWNRFLPKLLSAT
DmAChE  AARCSFWNDYLPKVRSWA
TcAChE  VQMCVFWNQFLPKLLNAT
```

Selection of template for homology modeling

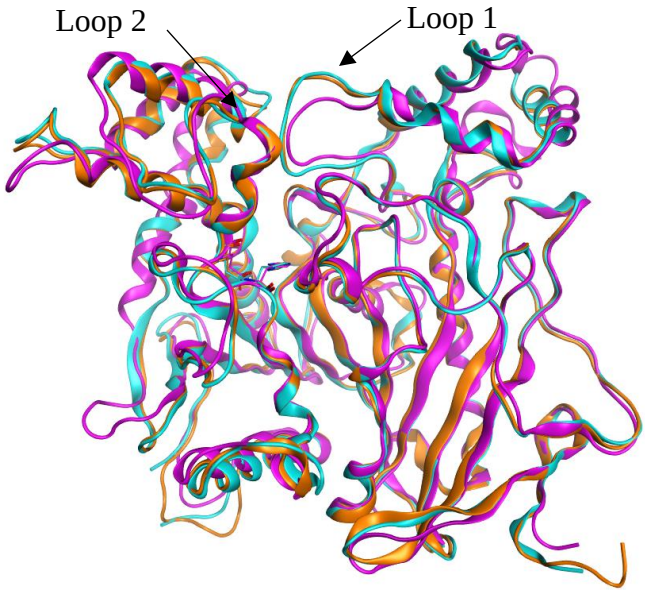

Figure S20. Superposition of *m*AChE (pdb code 5FOQ[5]; ribbon in orange), *h*AChE (pdb code 4EY4[6]; ribbon in cyan), or *Dm*AChE (pdb code 1DX4[7]; ribbon in magenta). The side chains of the amino acids in the catalytic triad are shown as sticks. AChE from three species were considered as template for the homology modeling, *m*AChE, *h*AChE, or *Dm*AChE. After the multiple alignments, the identity of the possible templates *m*AChE, *h*AChE, and *Dm*AChE and the sequences to be modelled were 48%, 48%, and 39% for *Ag*AChE1, respectively, and 48%, 48%, and 38% for *Aa*AChE1, respectively based on residues 1-543 in *h*AChE. One crystal structure from each species were superposed and visually analyzed. The analysis showed that both the general fold and the amino acids lining the active site are highly conserved among the different species. It could however be seen that the two loops at the entrance of the active site differs between *Dm*AChE and the vertebrate AChEs. In more details, 'loop 1' is one residue longer and 'loop 2' is two residues shorter. The multiple sequence alignment showed that for *Ag*AChE1 and *Aa*AChE1 'loop 2' contains the same number of residues as *Dm*AChE, but that 'loop 1' is one residue shorter (i.e. three residues shorter than vertebrate AChE). Although showing a lower sequence identity, *Dm*AChE (pdb 1DX4[7]) was selected as the main template, due to the higher similarity of 'loop 1' and 'loop 2'. This template was used to model all residues with the exception of three loops: 102-112, 487-499, and 512-520 (*h*AChE numbering). It was found that in 1DX4 these loops were either not modelled or that their lengths differed from *Ag*AChE1 and *Aa*AChE1, resulting in *m*AChE (pdb code 5FOQ)[5] being considered as a more suitable template for modelling of these residues.

Angles of Tyr337 in homology models of *Ag*AChE1 and *Aa*AChE1

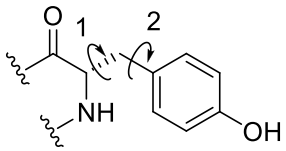

Figure S21. χ_1 (C_α-C_β) and χ_2 (C_β C_1) dihedral angles for the side chain of Tyr337 (*h*AChE numbering) were adjusted to -157.0 and -157.1 degrees and χ_2 (C_β C_1) -26.4 and -26.3 degrees for *Ag*AChE1 and *Aa*AChE1, respectively. These angles resemble those in **2**•*m*AChE and have been observed in previously reported protein-ligand complexes of *m*AChE and *h*AChE (for examples see complexes with pdb codes 4ARB[8] and 4EY7[6]).

Evaluation of *Ag*AChE1 and *Aa*AChE1 homology models

Table S9. Statistics of the stereochemical quality of the generated homology models according to PROCHECK.[9]

Ramachandran plot no. of residues (%)	***Ag*AChE1**	***Aa*AChE1**
Most favoured regions	364 (81.3)	368 (81.8)
Additional allowed regions	73 (16.3)	73 (16.2)
Generously allowed regions	7 (1.6)	4 (0.9)
Residues in disallowed regions	4 (0.9)	5 (1.1)

Compounds **1** and **2** modelled into the active site of *Ag*AChE1 and *Aa*AChE1.

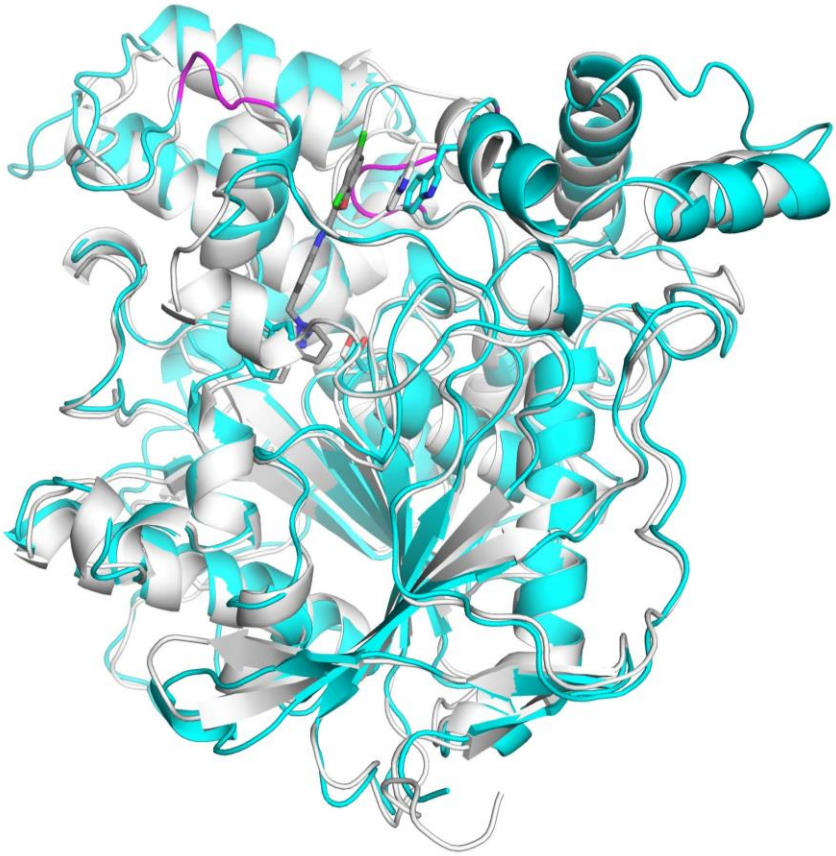

Figure S22. Superposition of the homology model of *Ag*AChE1 (cyan ribbon) and *m*AChE (gray ribbon) in complex with **1** (dark gray). The differing loops (loop 1 and loop 2) at the entrance of the gorge of *Ag*AChE1 are marked in magenta.

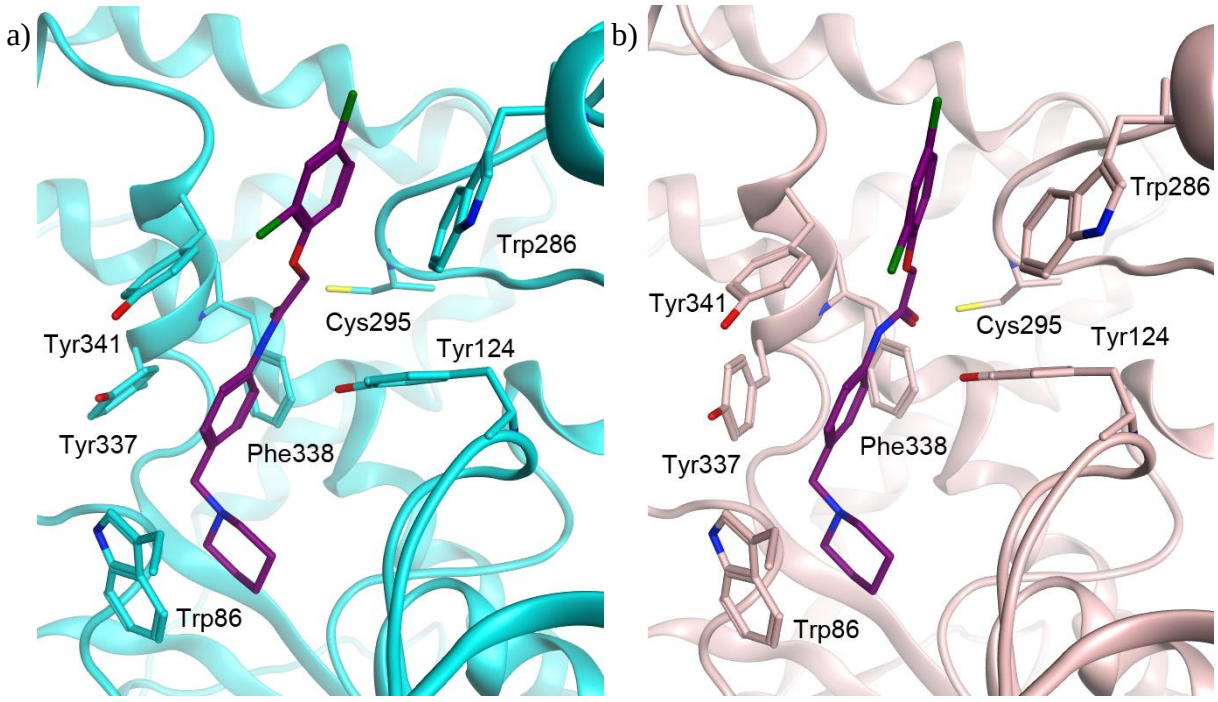

Figure S23. Homology model of *Ag*AChE1 in cyan (a) and *Aa*AChE1 in pink (b) showing a close up of active site with **1** (purple) modelled with the positively charged piperidine projecting down into the catalytic site (based on **1**•*m*AChE).

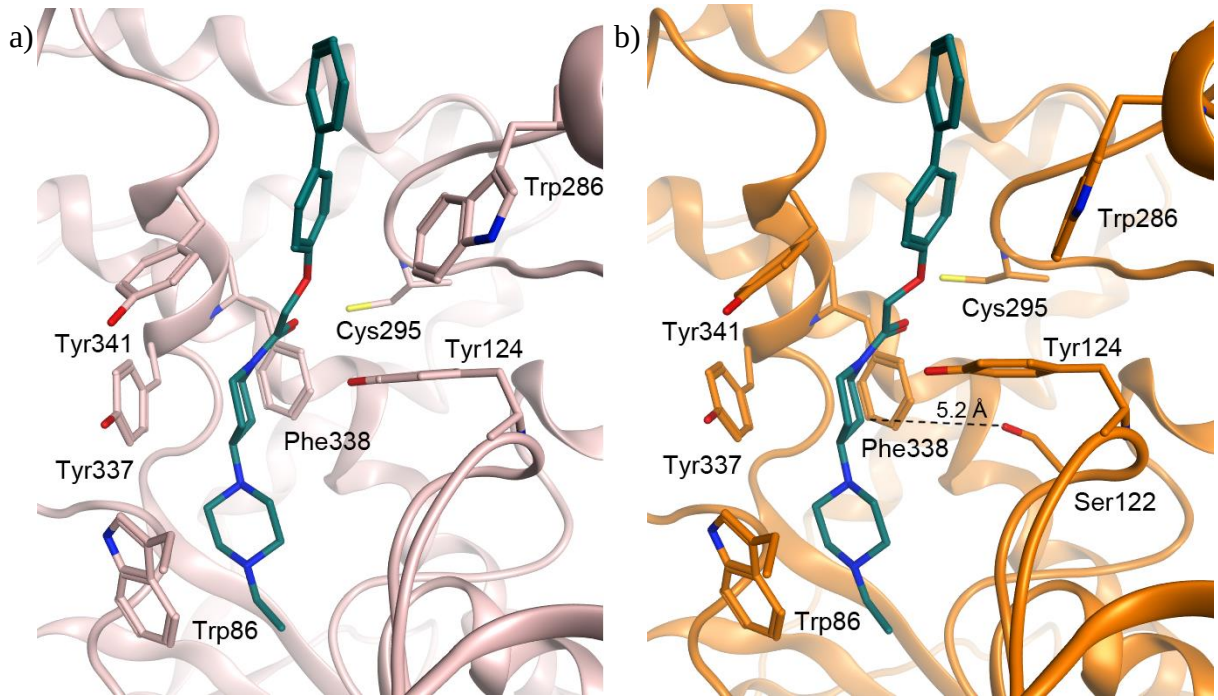

Figure S24. Homology models of *Aa*AChE1in pink (a) and of G122S-*Ag*AChE1 in orange (b) showing a close up of active site with **2** (green) modelled with the positively charged piperazine projecting down into the catalytic site (based on **2** aligned on **1**•*m*AChE).

Data collection and refinement statistics for 5FUM

Table S10. Data collection and refinement statistics for 5FUM. Statistics for the highest-resolution shell are shown in parentheses.

pdb entry code	5FUM
Resolution range (Å)	29.08 - 2.5 (2.59 - 2.5)
Space group	P 21 21 21
Unit cell (Å)	78.7 × 110.8 × 227.6
Total reflections	520714 (51599)
Unique reflections	69320 (6799)
Multiplicity	7.5 (7.6)
Completeness (%)	99.60 (99.28)
Mean I/sigma(I)	14.69 (2.35)
Wilson B-factor (Å^2)	51.2
R-merge	0.124 (1.584)
R-meas	0.1333 (0.724)
CC1/2	0.998 (0.885)
CC*	0.999 (0.969)
R-work	0.196 (0.3103)
R-free	0.227 (0.3888)
Number of non-hydrogen atoms	8602
macromolecules	8350
ligands[a]	123
water	129
Protein residues	1068
RMSD from ideal values	
bond lengths (Å)	0.004
bond angles (°)	0.89
Ramachandran favored (%)	95
Ramachandran outliers (%)	0.28
Clashscore	0.72
Average B-factor (Å^2)	62.00
macromolecules	61.60
ligands	87.50
solvent	58.90

[a]These include compound **2** (modelled in both the A and the B chain) and fragments of six PEG750MME molecules modelled in the structure.

References

1. Berg, L.; Andersson, C. D.; Artursson, E.; Hörnberg, A.; Tunemalm, A.-K.; Linusson, A.; Ekström, F. Targeting acetylcholinesterase: Identification of chemical leads by high throughput screening, structure determination and molecular modeling. *PLoS One* **2011**, *6*, e26039.
2. *SIMCA-P+*, version 13.0.3; Umetrics AB: Box 7960, Umeå, Sweden, 2013.
3. *Molecular Operating Environment (MOE)*, version 2012.10; Chemical Computing Group Inc.: 1010 Sherbooke St. West, Suite #910, Montreal, QC, Canada, H3A 2R7, 2012.
4. Larkin, M. A.; Blackshields, G.; Brown, N. P.; Chenna, R.; McGettigan, P. A.; McWilliam, H.; Valentin, F.; Wallace, I. M.; Wilm, A.; Lopez, R.; Thompson, J. D.; Gibson, T. J.; Higgins, D. G. Clustal W and Clustal X version 2.0. *Bioinformatics* **2007**, *23*, 2947-2948.
5. Berg, L.; Mishra, B. K.; Andersson, C. D.; Ekström, F.; Linusson, A. The nature of activated non-classical hydrogen bonds: A case study on acetylcholinesterase-ligand complexes. *Chemistry* **2016**, *22*, 2672-2681.
6. Cheung, J.; Rudolph, M. J.; Burshteyn, F.; Cassidy, M. S.; Gary, E. N.; Love, J.; Franklin, M. C.; Height, J. J. Structures of human acetylcholinesterase in complex with pharmacologically important ligands. *J. Med. Chem.* **2012**, *55*, 10282-10286.
7. Harel, M.; Kryger, G.; Rosenberry, T. L.; Mallender, W. D.; Lewis, T.; Fletcher, R. J.; Guss, J. M.; Silman, I.; Sussman, J. L. Three-dimensional structures of *Drosophila melanogaster* acetylcholinesterase and of its complexes with two potent inhibitors. *Protein Sci.* **2000**, *9*, 1063-1072.
8. Berg, L.; Niemiec, M. S.; Qian, W.; Andersson, C. D.; Wittung-Stafshede, P.; Ekström, F.; Linusson, A. Similar but different: thermodynamic and structural characterization of a pair of enantiomers binding to acetylcholinesterase. *Angew. Chem., Int. Ed.* **2012**, *51*, 12716-12720.
9. Laskowski, R. A.; Macarthur, M. W.; Moss, D. S.; Thornton, J. M. PROCHECK: A program to check the stereochemical quality of protein structures. *J. Appl. Crystallogr.* **1993**, *26*, 283-291.